

NASA

ELECTROLUMINESCENT LIGHT SOURCES

By R. O. Bell, S. C. Foote, C. B. Lamport, A. A. Menna, and G. A. Wolff

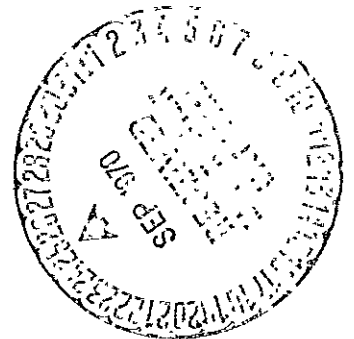
July 1970

Distribution of this report is provided in the interest of information exchange and should not be construed as endorsement by NASA of the material presented. Responsibility for the contents resides with the organization that prepared it.

Prepared under Contract No. NAS 12-2044 by

Tyco Laboratories, Inc.
Waltham, Massachusetts 02154

Electronics Research Center
National Aeronautics and Space Administration



FACILITY FORM 602

N70-41105
(ACCESSION NUMBER)

60
(PAGES)

CR-113907
(NASA CR OR TMX OR AD NUMBER)

1
(CODE)

26
(CATEGORY)

Reproduced by
NATIONAL TECHNICAL
INFORMATION SERVICE
Springfield, Va. 22151

Dr. James D. Childress, Code RMM
Technical Monitor
NASA, Electronics Research Center
Component Technology Laboratory
575 Technology Square
Cambridge, Massachusetts 02139

Requests for copies of this report should be referred to:

NASA Scientific and Technical Information Facility
P. O. Box 33
College Park, Maryland 20740

NASA

ELECTROLUMINESCENT LIGHT SOURCES

By R. O. Bell, S. C. Foote, C. B. Lamport, A. A. Menna, and G. A. Wolff

July 1970

Final Technical Report

Prepared under Contract No. NAS 12-2044 by

TYCO LABORATORIES, INC.
Waltham, Massachusetts 02154

Electronics Research Division
NATIONAL AERONAUTICS AND SPACE ADMINISTRATION

FOREWORD

This report covers work performed under Contract No. NAS 12-2044 from 1 November 1968 to 30 September 1969. The aim of this program was the selection of a solid solution of two III-V compounds, superior to present $\text{GaAs}_x\text{P}_{1-x}$ systems, based on its potential for use as electroluminescent light sources with emission in the 5000 to 6500 Å range, good visibility, and high efficiency at room temperature. Further, the goal of the program included optimization of this material for application to and production of electroluminescent diodes.

The work was administered under the direction of NASA, Electronics Research Center, Component Technology Laboratory, Cambridge, Massachusetts, with Dr. James D. Childress as Technical Monitor. Work under this contract was carried out at Tyco Laboratories, Inc., Waltham, Massachusetts, under the technical direction of Dr. Gunther A. Wolff, Principal Scientist. Tyco personnel contributing to the task under this program were:

Dr. R. O. Bell, Senior Scientist (electronic and optical data)

Miss S. C. Foote, Staff Scientist I (X-ray data and electrical contacting)

Mr. C. B. Lamport, Principal Experimental Assistant (material preparation and crystal growth)

Mr. A. A. Menna, Staff Scientist I (material preparation and crystal growth).

The technical advice and personal interest of Dr. A. I. Mlavsky, Director of the Corporate Technology Center, and Mr. F. Wald, Head of the Materials Science Department, are gratefully acknowledged. Thanks are also due to Miss C. Raith, Staff Scientist II, for crystal growth work in the terminal phase of the contract.

Table of Contents

Section	Page No.
SUMMARY	1
INTRODUCTION	1
EXPERIMENTAL TECHNIQUES	5
Basic Principles of THM Growth	5
Crystal Growth Experiments	7
General Remarks	7
Temperature and Growth Rate	7
Crystal Growth Furnace	7
Ampoule Material and Design	7
Form of Feed	12
Solvent	12
Commentary on Experimental Results in Crystal Growth	12
Remarks	12
Separation of Feed Material From the Liquid Solvent Zone and Preventive Measures	12
Sample Appearance	16
Materials Evaluation	16
X-Ray Analysis: Measurement of Composition	16
X-Ray Analysis: Experimental Methods	18
Comparison of Optical and X-Ray Data Obtained on $Ga_xIn_{1-x}P$	23
CONCLUSIONS AND RECOMMENDATIONS	24
REFERENCES	25
Appendix A: SOLUTION GROWTH OF ELECTRONIC COMPOUNDS AND THEIR SOLID SOLUTIONS	27

Table of Contents (Cont.)

Section	Page No.
Appendix B: ON SOLUTION AND TRAVELLING SOLVENT ZONE GROWTH OF SEMICONDUCTING COMPOUNDS AND SOLID SOLUTIONS	45
Appendix C: ANALYSIS OF CRYSTAL ORIENTATION	47
Appendix D: ELECTRICAL CONTACTING	51

List of Illustrations

Figure No.		Page No.
1.	Energy Gap of GaP-InP Alloy System as Function of Composition	3
2.	Schematic of THM Crystal Growth Apparatus (a) at Beginning of Growth and (b) at Later Stage	6
3.	Variable Speed Crystal Growth Apparatus, 0 to 12 mm/Day	10
4.	Schematic of Apparatus for Crystal Growth By Travelling Heater Method	11
5.	Sliced Charge From Growth Experiment No. 5 Showing Solvent in Two Slices on Right and In Center Section of Third Slice From Left	13
6.	Axially Sliced Crystal From Growth Experiment No. 10	13
7.	Charge of Crystal Growth Run No. 11 After Completion of Experiment	13
8.	Sliced Crystal No. 11	14
9.	Slices of Crystal From Experiment No. 22	14
10.	Schematic Illustrating the Use of Solid Rods of GaP and InP as Feed Material in Crystal Run No. 11	17
11.	Variation of Lattice Parameter With Composition Illustrating the Correction to Vegard's Rule Introduced By the Zen Relationship	19
12.	Calculation of Lattice Parameter of Inhouse InP.	19
13.	Band Gap Energy As Determined By Optical Transmission at Various Positions For Slice No. 5, Run No. 2	22
14.	Energy Gap of $Ga_xIn_{1-x}P$, Run No. 10	22

ELECTROLUMINESCENT LIGHT SOURCES

By R. O. Bell, S. C. Foote, C. B. Lamport, A. A. Menna, and G. A. Wolff

Tyco Laboratories, Inc.
Waltham, Massachusetts 02154

SUMMARY

$\text{Ga}_x\text{In}_{1-x}\text{P}$, of composition $0.6 \lesssim x < 0.8$, was selected from the various solid solutions of III-V compounds as the most promising material for an electroluminescent light source which would emit in the visible 5000- to 6500-Å range. Solid crystal ingots 0.8 cm in diameter and up to 2.2 cm in length, of composition $0 \lesssim x \lesssim 0.8$, have been grown by the traveling heater method (THM).

In this method, a molten $\text{Ga}_y\text{In}_{1-y}$ solvent zone is moved, at a rate of 3 mm/day and a temperature of 1000 to 1050 °C, through a loosely packed $(\text{GaP})_x(\text{InP})_{1-x}$ feed mix or through a GaP-InP couple of parallel, aligned crystal rods. For the growth of solid solution crystals of 37 and 70 mol % GaP content, respectively, solvent alloys of initial GaP content of 20 and 35 mol % Ga were used. An exploratory experiment indicated the feasibility of seeding with GaP crystals.

The fabrication of sufficiently compact and uniform solid solution ingots which were to be used as the ideal feed material for regrowth in later experiments was the ultimate reason for the initial use of the substitute feeds mentioned. Within this initial limitation, the quality and reproducibility of the material obtained was indeed impressive.

Optical transmission data taken from separate samples showed axial as well as radial homogeneity. An axial homogeneity of 41 ± 1 mol % GaP over the tested two-thirds of an 18 mm region was found for one sample, while the major part of the cross section of another sample showed a composition of 53 ± 0.3 mol % GaP. X-ray measurements confirmed the general composition range determined optically.

A new technique for the rapid determination of {111}-twinned grains in the unseeded growth of (Ga, In)P has been derived. This technique shows promise as a substitute for the cumbersome and time consuming Laue method, and should reduce the prohibitive time factor in the type of study that is necessary for the optimization of single crystal growth of zinc-blende or other fcc materials.

INTRODUCTION

The optical and electrical properties of each III-V compound are characteristics of that compound which can only be varied to a limited degree by doping. Therefore, the possibility of making solid solutions of semiconducting compounds having varied intrinsic properties, such as a band gap energy lying between those of the simple III-V compound end members, is of interest.

The purpose of this contract was the optimization of production techniques for a red-orange electroluminescent diode, made from a solid solution of semiconducting III-V compounds, which would be superior to present Ga(As,P) devices. This aim required the selection and preparation of a high quality material of an acceptable, alternate solid solution

system as well as a refinement of techniques for the manufacture of controlled and reproducible diodes.

The $\text{Ga}_x\text{In}_{1-x}\text{P}$ system appears to be best suited for this task. M. R. Lorenz, et al., (Ref. 1) showed it to be a direct bandgap semiconductor within the large (0 to 80 mol % GaP) composition range shown in Fig. 1. In addition, external quantum efficiencies of up to 7.2% have been obtained for GaP red light-emitting diodes (Ref. 2). Therefore, although indirect materials are normally less efficient than direct semiconductors (Ref. 3), there is the distinct possibility that acceptable efficiencies might also be obtained in indirect bandgap materials, especially in (Ga, In)P containing 80 mol % or more GaP. Furthermore, in this system one would not anticipate any of the serious corrosion or oxidation problems of the type encountered in the respective aluminum compounds and their solid solutions.

The most efficient light-emitting III-V compound diodes (including laser diodes) obtained so far, as well as the red light-emitting GaP diode mentioned, were prepared from their metallic solutions by normal growth and liquid epitaxy. It was, in fact, in solution grown material that the current and electron beam induced electroluminescence in GaP and its solid solutions with GaAs and InP was first observed and reported by this writer (Ref. 4 and 5). In the light of these findings, it is only natural to choose solution growth methods for the preparation of GaP-InP solid solutions and also for the fabrication of electroluminescent diodes made from these solid solutions.

For the bulk growth of $\text{Ga}_x\text{In}_{1-x}\text{P}$ crystals (for use as an efficient electroluminescent light source material), the traveling heater method (THM) was used. Previously, this technique had been successfully applied to the growth of a wide variety of compounds and solid solutions. These are listed in Appendix A, Table I, and include GaP, GaAs, Ga(As,P), HgTe, (Hg, Zn)Te, CdTe, CdCr_2Se_4 , (Pb, Sr)TiO₃, CuCl, and others. In particular, THM growth ensures macroscopic homogeneity of solid solutions by its steady-state growth mechanism, while at the same time it effectively minimizes their microscopic inhomogeneity due to temperature fluctuations by its diffusion controlled material transport. In this method, thermally induced transient change in material composition and deposition rate is almost instantaneously slowed down by the resisting momentum of solute diffusion to the interface of the growing crystal.

Initially, solid crystal ingots of approximate composition $\text{Ga}_{0.4}\text{In}_{0.6}\text{P}$ were grown by THM from a solution in Ga-In solvent. During the course of this work, it was reported in the literature (Ref. 1) that electroluminescence from $\text{Ga}_x\text{In}_{1-x}\text{P}$ diodes due to direct band to band recombination could be obtained for values up to $x \approx 0.80$ instead of $x \approx 0.63$, as estimated from previous studies (Ref. 6). Therefore, x was raised to approximately 0.75 by changing all of the respective growth conditions in a single step.

This approach is normally not recommended, but it was taken because of limits in time and level of efforts. However, the result obtained showed that, despite the increased complexity and more stringent requirements of the phase diagram for the solid solution-liquid solution system (as compared to those of singular compounds), conditions of solid solution growth could be successfully predicted.

In the following sections, the basic principles and experimental design of the THM for the growth of (Ga, In)P crystals will be given in detail. Also included is a Data Table for all experiments performed. X-ray and optical transmission measurements will then be described

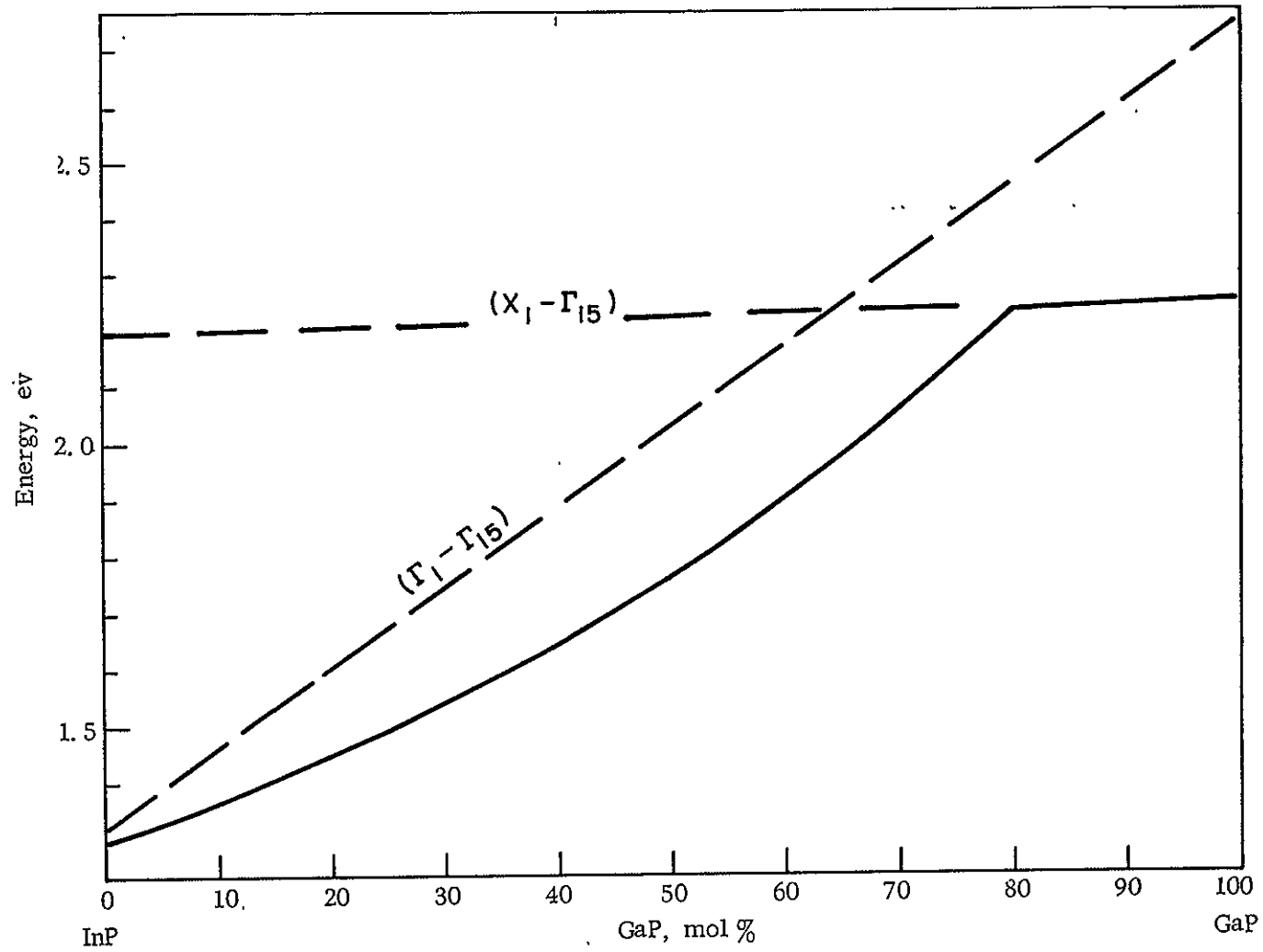


Fig. 1. Energy gap of GaP-InP alloy system as function of composition [broken lines are extrapolated energy levels assuming linear dependence on composition; after Lorenz, et al., Ref. 1].

and interpreted in terms of energy gap, composition, and homogeneity of the material obtained.

In addition to the general presentation, Appendix A outlines in some detail fundamental and practical principles of the crystal growth of semiconductor compounds and their solid solutions by the traveling heater method. Appendix B summarizes these results. Appendix C proposes a new technique for the rapid determination of crystal orientation in multiple grain growth by etching to elucidate the optimal growth and nucleation processes. Appendix D describes a study of electrical contacting and a proposed technique for its improvement.

EXPERIMENTAL TECHNIQUES

Basic Principles of THM Growth

In crystal growth by the so-called traveling heater method (THM), a molten zone that is in equilibrium with the crystal composition to be grown is made to migrate through a polycrystalline source material of desired composition by slow movement of either the heater or the charge (Fig. 2). The dissolution of feed material occurs at the advancing (hot) liquid-solid interface, and crystallization of the solid solution, $\text{Ga}_x\text{In}_{1-x}\text{P}$, occurs at the receding (cool) liquid-solid interface. The composition versus temperature phase equilibrium determines the optimum solvent temperature, and the liquid diffusion rate of the compound in the solvent determines the maximum feasible growth rate.

A simplified analysis of heat and material transport (including the proper adjustment of the temperature distribution along the liquid solution zone axis to eliminate the instability of the crystal growth front by constitutional supercooling) in crystal growth by THM was presented in four recent papers (Refs. 7 through 9, and Appendix A).

Some of the advantages of this type of crystal growth technique for a solid solution such as $\text{Ga}_x\text{In}_{1-x}\text{P}$ are:

1. Compared with other growth techniques, crystals of higher perfection are obtained.
2. Precise control of the composition is obtained by controlling the composition of the feed material and allowing the growth to continue long enough to approach equilibrium.
3. Purification of the crystal will occur if the segregation coefficient of the impurities in the solid relative to the solvent is less than one.
4. Contamination from the crucible material will be reduced because of the lower growth temperatures, which also makes the problem of finding suitable containers easier.
5. The equipment, including the heat source and temperature controller, is quite simple and requires little attention while in operation.

By adjusting the length of the solution zone, rate of movement, solvent temperature, and temperature gradient at the interface, one is able to control and optimize the crystal growth conditions. To a great extent, the rate of material diffusion within the solution zone limits the rate of crystal growth to a maximum value of approximately 5 to 8 mm/day. Any attempt to increase the crystal growth rate above the critical value will be detrimental to single crystal growth; however, thermal convection may contribute to an increase of the maximum growth rate in some instances.

Although inferior crystal ingots can be grown when the solution is constitutionally supercooled, this effect should and can be avoided in order to improve crystal growth and perfection, and in order to preclude solvent and impurity entrapment. Constitutional supercooling is eliminated by adjusting the temperature and the temperature profile of the zone so that the solute solubility (i. e., saturation concentration) gradient towards the zone center exceeds the actual solute concentration gradient within the entire zone, and crystallization is only possible at the growth front. In this way, the stability of both liquid-solid interfaces at the opposite zone ends is established. The potential growth rate of any seed or feed material protruding

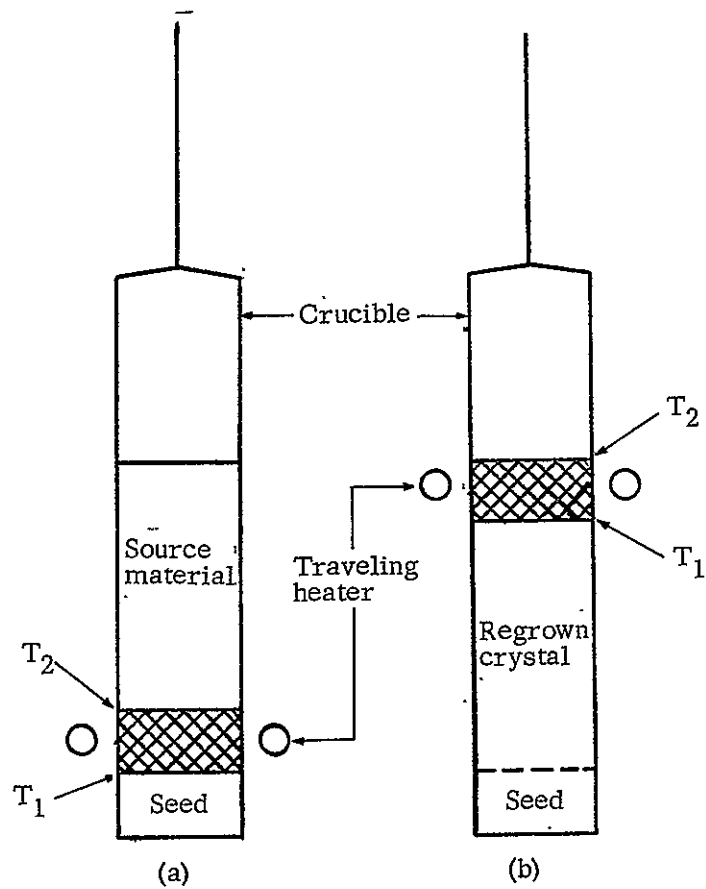


Fig. 2. Schematic of THM crystal growth apparatus (a) at beginning of growth and (b) at later stage

into the solution, or of any seed material accidentally or otherwise introduced into the liquid zone, does not increase towards the zone center.

Crystal Growth Experiments

General remarks:--Table I summarizes the growth conditions of the various experiments and the results obtained. At the beginning of the period of experimental work on this contract, it was assumed, in lieu of experimental evidence, that the width of the band-gap varied linearly with the composition of the solid solution. Therefore, following the results presented in Ref. 6, the desired composition range in the $\text{Ga}_x\text{In}_{1-x}\text{P}$ system for emission in the required range was originally $0.3 < x < 0.4$. For the first 13 crystal runs, the growth of $\text{Ga}_{0.37}\text{In}_{0.63}\text{P}$ was attempted. However, Lorenz, et al. (Ref. 1), published an experimental determination of band-gap as a function of composition (see Fig. 1), which showed that this function was extremely nonlinear. Thus, in remaining crystal runs (nos. 14 through 32), efforts were concentrated on the growth of $\text{Ga}_{0.70}\text{In}_{0.30}\text{P}$.

The ternary phase diagram (Ga-In-P) was also not established at the time, so growth parameters could not be derived [work in this field has since been done by M. Panish (Ref. 10)]. Therefore, combining knowledge of the Ga-In, Ga-P, and In-P binaries with knowledge of similar ternaries, e. g., Ga-Al-As, we chose estimated growth parameters.

Growth variables in THM include feed composition, solvent composition, solvent zone temperature and gradient, and growth rate. After fixing the feed composition at the desired crystal composition, we made an educated guess as to solvent composition. For a feed of $\text{Ga}_{0.37}\text{In}_{0.63}\text{P}$, this was adjusted to be $\text{Ga}_{0.20}\text{In}_{0.80}$. Later, when the feed composition changed to $\text{Ga}_{0.70}\text{In}_{0.30}\text{P}$, the solvent Ga:In ratio was changed to 35:65, accordingly.

Temperature and growth rate. --Since the melting points of both constituents are high, the highest temperatures ($\approx 1000^\circ\text{C}$) possible were used in the experimental furnaces. The growth rate chosen was a compromise between the desire to allow diffusion to make the crystal grown as homogeneous as possible and the practical need to evaluate experimental parameters after several days. Therefore, 3 mm/day was the rate used for 8-mm ampoules. Lower rates were used for higher diameter ampoules. In one case (crystal run no. 12), a higher rate was used to determine if an upper limit on growth rate existed. The furnace design is described in the following paragraphs.

Crystal growth furnace. --Fig. 3 is an assembly drawing of the furnace being used for single crystal growth by THM at Tyco. The solvent zone heater located opposite the viewing port is wound with Kanthal A-1 (0.032-in. diameter) resistance wire on the alumina muffle. The precision mechanical drive mechanism allows accurate and uniform lowering of the ampoule (which contains the feed material, solvent zone, and growing crystal) through the hot zone. Either a chromel-alumel or a platinum-platinum plus 13% rhodium thermocouple is placed in thermal contact with the heating element and used with a temperature controller to maintain uniform thermal conditions during the long (1 to 2 weeks) growth period. Fig. 4 is a schematic view of the growth furnace in operation.

Ampoule material and design. --Quartz ampoules were used in view of the high growth temperatures and the possibility of the solvents attacking the ampoule material. Early ampoule design consisted of flat bottom, 8-mm-i. d. tubes with quartz rods attached to the bottom. The quartz rods simulate the heat drain of the feed above the solvent zone in the opposite direction.

TABLE I
EXPERIMENTAL CONDITIONS AND RESULTS FOR THE VARIOUS GROWTH RUNS

Run No.	Duration, days	Feed Composition, mole fraction	Solvent Composition, atomic fraction	Temperature, °C	Growth Rate, mm/day	Amount Regrowth, mm	Preparation	Comments		
1	21	$\text{Ga}_{0.37}\text{In}_{0.63}\text{P}$	$\text{Ga}_{0.20}\text{In}_{0.80}$	~840	1	2	Feed: 100-mesh powder in pressed pellets	—		
2	18	↓	↓	950	2	13	First two feed pellets enriched with solvent material; last two as before	Growth ceased at interface between solvent enriched and nonenriched pellets		
3	12			1000	3	2	Feed powder mixed with material of solvent composition and pressed into pellets	Drive mechanism failure		
4	4			959	—	—	Furnace burned out			
5A	10			981	—	—	Drive mechanism in reverse			
5B	9			981	12	—	—			
6A	<1			1002	—	—	Furnace burned out			
6B	6			1002	3	—	Separation of feed from solvent zone			
7	7			991	6	—	Feed: 100-mesh loose powder	Separation of feed from solvent zone		
8	2			1002	—	—	Feed: pellets of 100-mesh powder mixed with material of solvent composition and grooved	Furnace burned out		
9	7			1002	2	5	Same as no. 8	Separation of feed from solvent zone		
10	8			991	3	18	Feed: 80-mesh loose powder	All feed consumed		
11	13			1005	2	14	Feed: solid rods of GaP and InP	Inhomogeneous regrowth		
12	5			1002	5	5	Feed: loose powder	Separation of feed from solvent zone		
13	13			1000	3	22	Feed: loose powder; solvent saturated with feed; seeded with polycrystalline GaP	—		
14	10			$\text{Ga}_{0.70}\text{In}_{0.30}\text{P}$	$\text{Ga}_{0.35}\text{In}_{0.65}$	1007	2	2	Feed: loose powder	Separation of feed from solvent zone
15	10			1000	3	—	Feed: loose powder; seeded by platelets of GaP oriented in {111} direction	Growth of platelets on seed		
16	10			1020	3	—	Feed: loose powder; self-seeding ampoule	No solvent zone movement; separation of feed from solvent zone		
17	10	1010	3	—	Feed: loose powder; solvent vacuum distilled	Separation of feed from solvent zone				

Table I (cont.)

Run No.	Duration, days	Feed Composition, mole fraction	Solvent Composition, atomic fraction	Temperature, °C	Growth Rate, mm/day	Amount Regrowth, mm	Preparation	Comments
18	12	$\text{Ga}_{0.70}\text{In}_{0.30}^{\text{P}}$	$\text{Ga}_{0.35}\text{In}_{0.65}$	1036	2	5	Feed: loose powder; solvent vacuum distilled	Separation of feed from solvent zone
19	3		$\text{Ga}_{0.35}\text{In}_{0.65}$	1040	3	—	Feed: loose powder; solvent vacuum distilled	Furnace burned out
20	10		$\text{Ga}_{0.35}\text{In}_{0.65}$	970	3	—	Feed: loose powder; low temperature phase of solvent	Separation of feed from solvent zone
21	8		$\text{Ga}_{0.20}\text{In}_{0.80}$	1000	3	10	Feed: loose powder	Separation of feed from solvent zone
22	18		$\text{Ga}_{0.35}\text{In}_{0.65}$	1010	1.5	15	Feed: loose powder; solvent vacuum distilled	Separation of feed from solvent zone
23	17			970	1.5	—	Feed: loose powder; solvent vacuum distilled	Separation of feed from solvent zone; platelet growth
24	10			970	3	4	Feed: pellets 2 mm narrower than ampoule; stacked to let gas escape.	Solvent zone did not move
25A	5			960		—	Feed: pellets 2 mm narrower than ampoule; stacked to let gas escape	Solvent zone did not move
25B	6			1010		—	Rerun of no. 25A	Solvent zone did not move
26	8			1000		5	Feed: loose powder; solvent purified and saturated with feed	Separation of feed from solvent zone
27	10			1010		3	Feed: loose powder; solvent purified	Separation of feed from solvent zone
28	9			1005		2	Feed: loose powder; solvent purified	Separation of feed from solvent zone
29A	3			1020	1.5	—	Powdered feed wet with solvent	Preheater used; separation of feed from solvent zone
29B	21			1043	1.5	6-9	Separated feed shaken down to contact solvent	Preheater used; separation of feed from solvent zone
30A	6			1003	3	—	Feed: first 2 cm loose powder, last 0.7 cm wet with solvent	Preheater and afterheater used; solvent zone did not move
30B	12			1033	3	2	No. 30A material plus 8 mm solvent; 10 mm feed transferred to new ampoule	Preheater used; solvent zone stopped moving

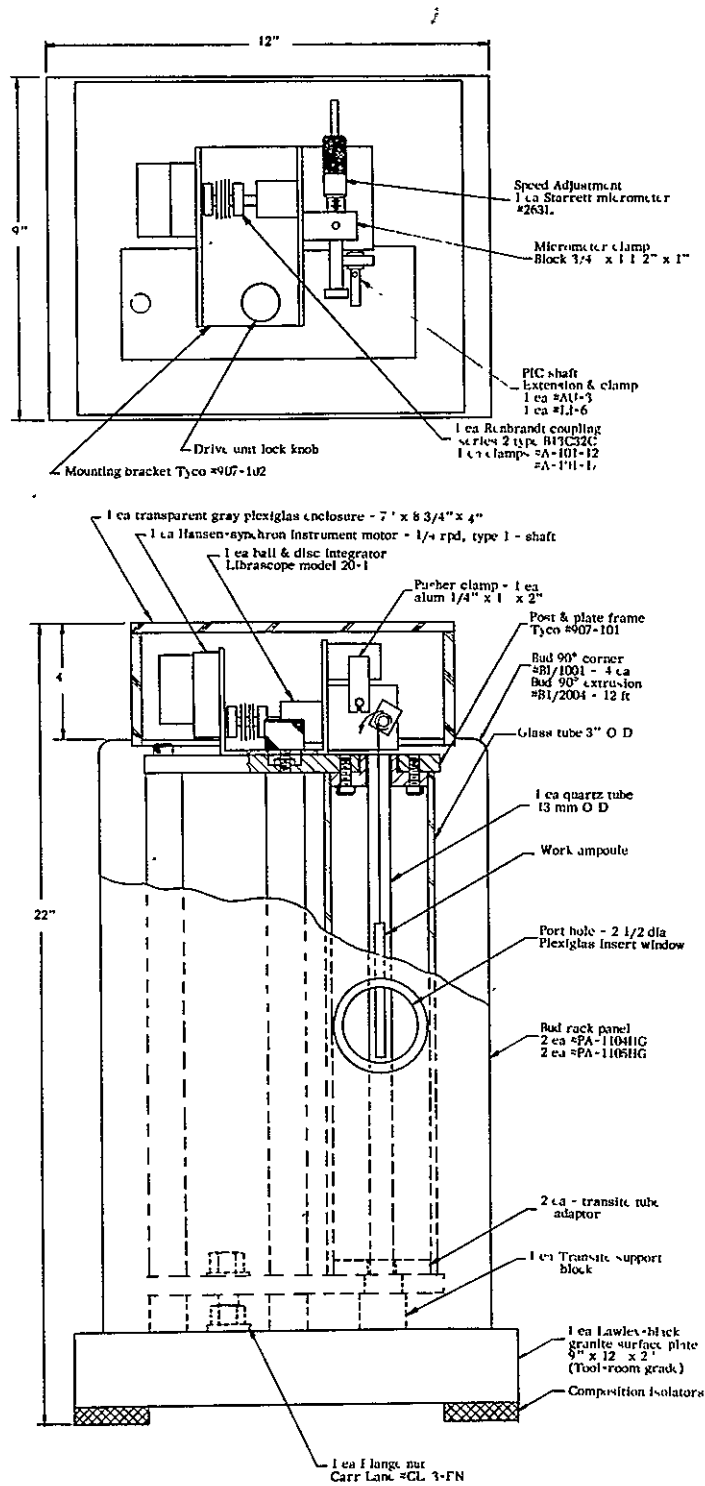


Fig. 3. Variable speed crystal growth apparatus, 0 to 12 mm/day
(Tyco drawing no. 907-100)

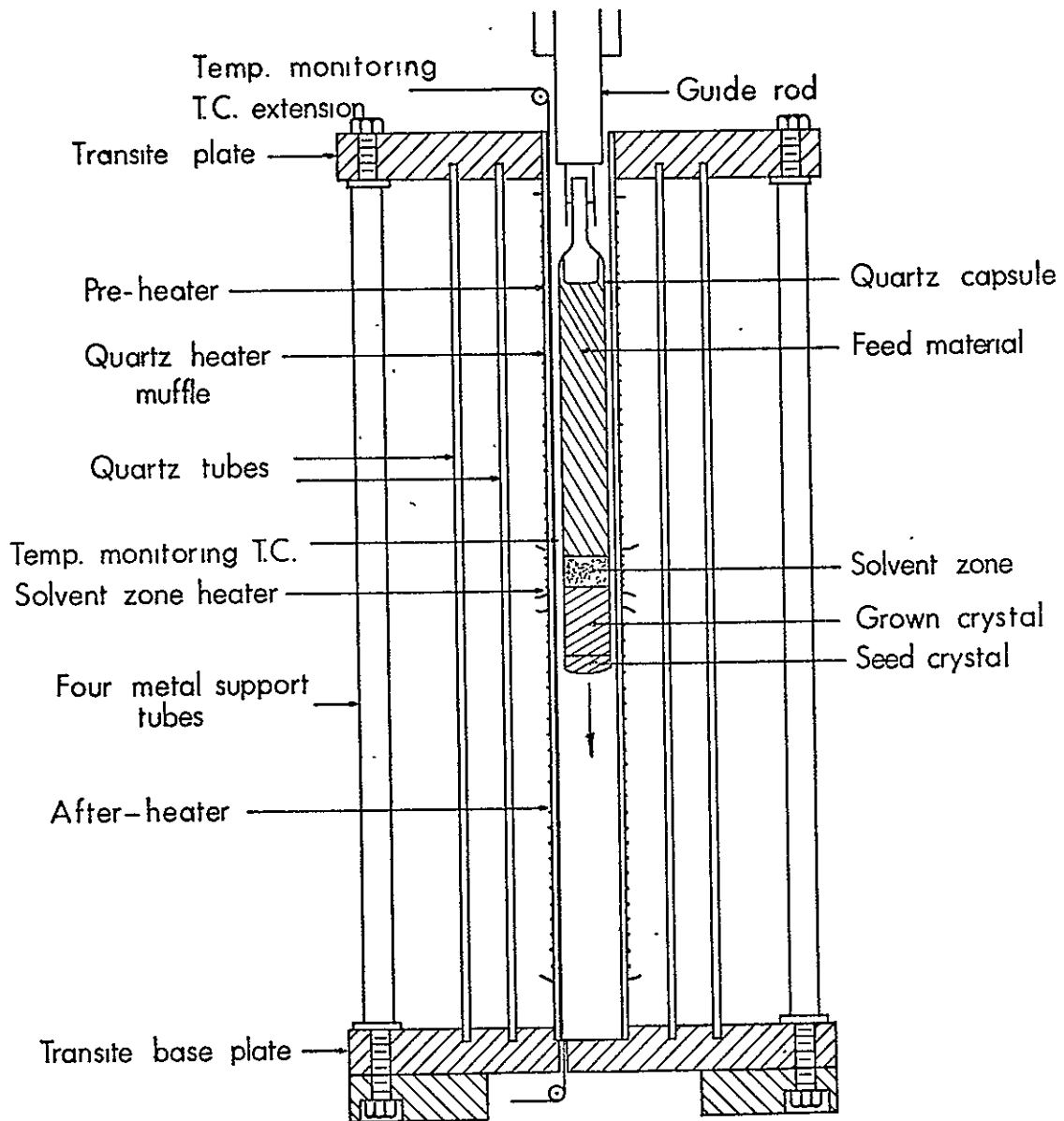


Fig. 4. Schematic of apparatus for crystal growth by travelling heater method

In some later runs, pointed or rounded-bottom tubes were used in an attempt to promote self-seeding.

Form of feed. -- Initially, 8-mm-diameter cylindrical pellets of fine powder of GaP and InP mixed in the proper proportions and pressed under 20,000 psi were used as feed. In some cases, the feed was saturated with the material of solvent composition. However, since crystal growth runs began to terminate because of separation of feed from solvent, it was decided to use loosely packed powder as feed, pellets that were smaller in diameter than the ampoule inner diameter, or solid rods of GaP and InP.

Solvent. -- During the experiments, it was found that the commercial "high purity" gallium source material (99.9999%) contained an appreciable amount of impurities, possibly oxides. It was therefore attempted to purify the metal by removing the volatile impurities at high temperatures under vacuum.

The gallium source material was placed in a quartz ampoule which was evacuated and heated to 1000 °C. A ring of volatile impurities (gray to black in color) formed on the inside wall of the ampoule above the metal (this had also been found in previous experiments). The tube was broken off the vacuum system, above the gallium but below the ring deposit, to avoid contact between the evaporated impurities and the gallium during its transfer to another tube. This procedure was then repeated; very little discoloration appeared on the inside wall of the quartz tube the second time. The purified gallium was then used as part of the gallium-indium solvent mixture for the crystal growth experiments following run no. 21.

Also, in some of the later growth experiments, gallium obtained from United Mineral Corp. was used in place of material from Alcoa. This gallium did not produce a black residue when vacuum treated as described above.

Commentary on Experimental Results in Crystal Growth

Remarks. -- The experimental conditions of the various growth runs and the results obtained were listed in Table I. Figs. 5 through 9 show some of the grown $\text{Ga}_x\text{In}_{1-x}\text{P}$ crystals.

Solid solutions of approximate composition $\text{Ga}_{0.4}\text{In}_{0.6}\text{P}$ (experiments nos. 1 through 13) were grown during the early phase of the contract to obtain reproducible results. The growth of solid solutions of higher GaP content was attempted in the second period. The higher GaP concentration was called for when it became known that electroluminescence due to direct band to band electron-hole transitions could be shifted toward shorter wavelengths (and the visible range) than was assumed before. Solid solutions of higher GaP content were obtained in these later experiments in 10 out of 19 growth runs (discounting furnace burn-out).

A reassignment of new personnel to this task and a short initial adjustment period may or may not have caused one of the growth runs to fail. One major detriment to growth, found and eliminated, was the presence of oxides and/or monophosphates in the solvent. Their removal greatly improved growth. Also, the furnace initially designed (sufficient for the growth of solid solutions of lower GaP content) appeared to provide a solvent zone temperature near its critical value but not in the safer range of 1000 to \approx 1050 °C. Thus, an increase in the furnace operating temperature (while maintaining the zone length at about 1.5 cm) should make the growth of large crystal ingots 90% reproducible.

Separation of feed material from the liquid solvent zone and preventive measures. -- In THM growth of solid single crystal ingots of $\text{Ga}_x\text{In}_{1-x}\text{P}$ a long polycrystalline ingot and a

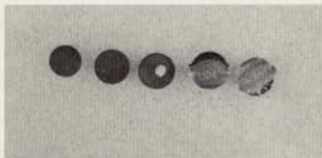


Fig. 5. Sliced charge from growth experiment no. 5 showing solvent in two slices on right and in center section of third slice from left (indicates concave solid-liquid interface; improved control of thermal flow in subsequent experiments resulted in essentially flat interfaces)

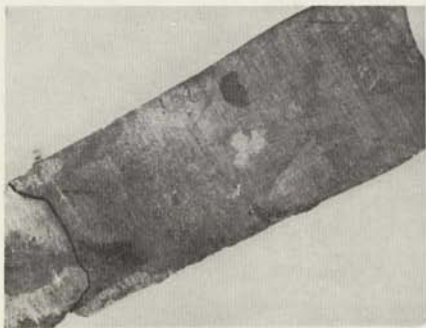


Fig. 6. Axially sliced crystal from growth experiment no. 10 (crystal is 18 mm long from bottom end at lower left to bound solidified solvent zone at upper right of marked interface; results from optical measurements on this crystal are shown in Fig. 14)

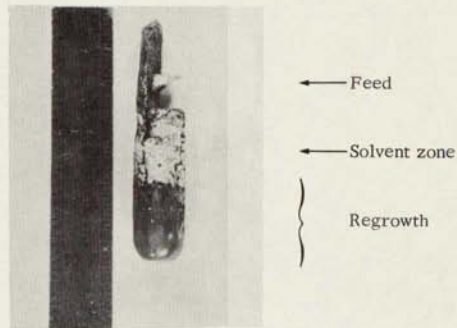


Fig. 7. Charge of crystal growth run no. 11 after completion of experiment [crystal grown from (GaP crystal + InP crystal) feed properly proportioned; remainder of GaP feed still visible; length of regrowth is 14 mm]



Fig. 8. Sliced crystal no. 11 (see Fig. 7)

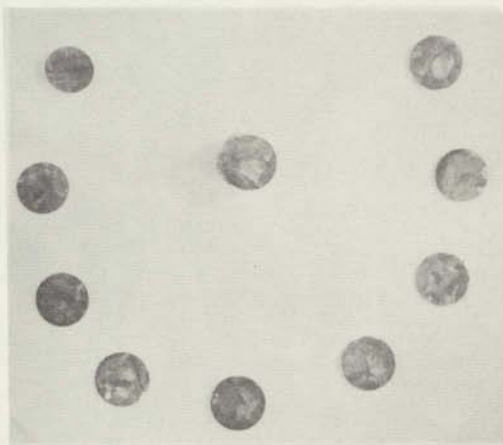


Fig. 9. Slices of crystal from experiment no. 22 (15 mm; growth occurred from left to right and center; note increased grain size)

shorter single crystalline ingot of this material would be ideal for use as feed and seed, respectively. Such a material could perhaps be prepared by rapid solidification of a molten mixture of $[x\text{GaP} + (1-x)\text{InP}]$ by quenching, by vapor phase growth using iodine as a transport agent, or else by another suitable method. Solid feed and seed $\text{Ga}_x\text{In}_{1-x}\text{P}$ ingots of fair homogeneity would facilitate the attainment of truly steady state THM growth conditions where identical amounts of material of identical composition would simultaneously dissolve as well as redeposit via the solution zone. However, within the set limits of projected efforts, this approach appeared to be impractical because of the experimental difficulties anticipated. For this reason, it was decided to grow solid $\text{Ga}_x\text{In}_{1-x}\text{P}$ ingots from powdered, pelleted $[x\text{GaP} + (1-x)\text{InP}]$ feed mixtures, or from axially-aligned GaP and InP solid rods. The resulting solid $\text{Ga}_x\text{In}_{1-x}\text{P}$ rods or "first preparations" could then be used (in a subsequent growth experiment) for a feed charge as well as for the yield of improved subsequent or "second preparations."

The experiments show that first preparations can indeed be grown in the way described. One problem was encountered, however, when powdered or pelleted GaP-InP feed mixtures were used. In a number of growth runs, the last portion of the feed material failed to transport through the solvent to the growing crystal. Upon a critical examination of the material and the remainder of the charge after termination of growth, it was concluded that, in these experiments, the microscopic pores present in the feed material were captured by the liquid zone and accumulated at its upper end during solvent zone passage through the feed. The accumulated "void" space within the upper region of the liquid zone then resulted in a narrowing of the effective solvent zone cross section through which diffusion or dissolution next to the feed crystal interface takes place.

Although the diffusion transport of solute and/or dissolution rate of feed material across this limiting constriction remains largely unchanged per unit area, the absolute amount of transported solute thus decreases nearly proportionally with decreasing cross-sectional area of the liquid zone constriction. The advance of the crystal growth front thus lags with respect to the dissolution front of the dissolving fraction of the feed material. As a consequence for constant rate of capsule movement, the distance between growth front and solution zone heater steadily increases until growth ceases eventually.

A closer study reveals that this detrimental effect on crystal growth can generally only occur for first crystal preparations (this is in contrast to second preparations where previously grown solid and compact feed crystals are used) where packed or pelleted feed material is applied. Excessively dense packing or high pressure pelleting induces the entrapment and accumulation of "void" space contrary to what one would normally expect. In dense packing or high pressure pelleting, the entrapped gases in the solid feed material are compressed to voids of negligible dimensions. When coming in contact with the liquid, the compressed gas in general immediately expands and escapes from the voids into the liquid zone.

Remedial measures may differ for different materials. The following approach has proved successful, however. It eliminates the accumulation of voids, or else promotes their continual removal through open void or liquid solvent channels to the space in the upper capsule end section by the use of the loosely packed or moderately pressed feed and solvent-feed mixtures.

In one experiment, another approach was used to eliminate the accumulation of voids between solution and feed and interruption of growth. Run no. 11 was specifically designed to

test the feasibility of using solid GaP and InP rods as feed material. The actual configuration used is illustrated in Fig. 10. Solid feed in this case was chosen for the following reasons:

1. Solid feed offers less surface area for contaminating adsorbants than powder, and eliminates pores in the powdered feed which are difficult to evacuate and thus may serve as contamination sources.
2. Solid feed eliminates porosity in the feed crystal, thus narrowing to smaller cross-sectional area the solution zone which in turn would inhibit crystal growth. The cross section of the solvent zone becomes smaller at the feed interface than at the crystal interface. Therefore, decreasing quantities of feed are dissolved, until the solvent is no longer saturated and precipitation of further crystalline material ceases. The constant quantity of material presented to the solvent zone by solid feed should solve the necking problem.
3. Finally, hindsight allows us to say that the free space present around the rods of feed material allows materials from solvent and feed to evaporate and condense on cooler portions of the ampoule. As we shall see later, if these evaporants are trapped by powdered feed, sufficient pressure may be built up to move the entire feed several millimeters or more up the tube, thus separating it from the solvent zone and stopping growth.

The disadvantage of using solid rods of GaP and InP as feed lies in the expected inhomogeneity of the resultant crystal. Phase diagram considerations imply that the InP rod will dissolve more rapidly than the other, and the equilibrium will not be reached for some time as the tube containing the charge travels through the heater. In addition, lack of even gross mixing in the feed will probably result in a nonequilibrium condition in a transverse section of the crystal. However, appropriate sectioning of the resultant crystal (longitudinally and transversely) and rearrangement of the sections (to place sections high in GaP next to others high in InP), followed by another pass through the furnace, should reduce these inhomogeneities.

Sample appearance. --A photograph of crystal no. 11 is shown in Fig. 7. The crystal consists of a transparent orange regrowth section 7 mm long topped by an opaque gray-black section approximately the same length. Gross optical examination shows that the lower layer is a GaP-rich solid solution, while the upper layer is rich in InP. The light colored section is the solvent zone. A remaining piece of solid feed 2 cm long can also be seen.

Optical inhomogeneity was also observed in sample no. 2, where transverse slices 1, 3, and 4 showed an opaque center surrounded by material of orange color. Slice no. 2 was completely transparent. Except for this growth section, the remainder of the ingot was of a uniform dark orange color. This result is also supported by the analysis of composition as described in the next section. In general, however, the other crystals prepared showed a uniform external appearance upon visual inspection. This would not be true for their bottom and top sections, which were orange and opaque, respectively.

This difference in composition at both crystal ends is only natural, since at the beginning and end of growth (i. e., when steady state growth conditions are not in effect), the composition of the deposit will deviate from the composition of the feed.

Materials Evaluation

X-ray analysis: measurement of composition. --One means of determining solution composition in the $\text{Ga}_x\text{In}_{1-x}\text{P}$ system is the identification of the lattice parameter, a_x , in the crystal. To a first approximation, it is commonly assumed that the relation between the lattice

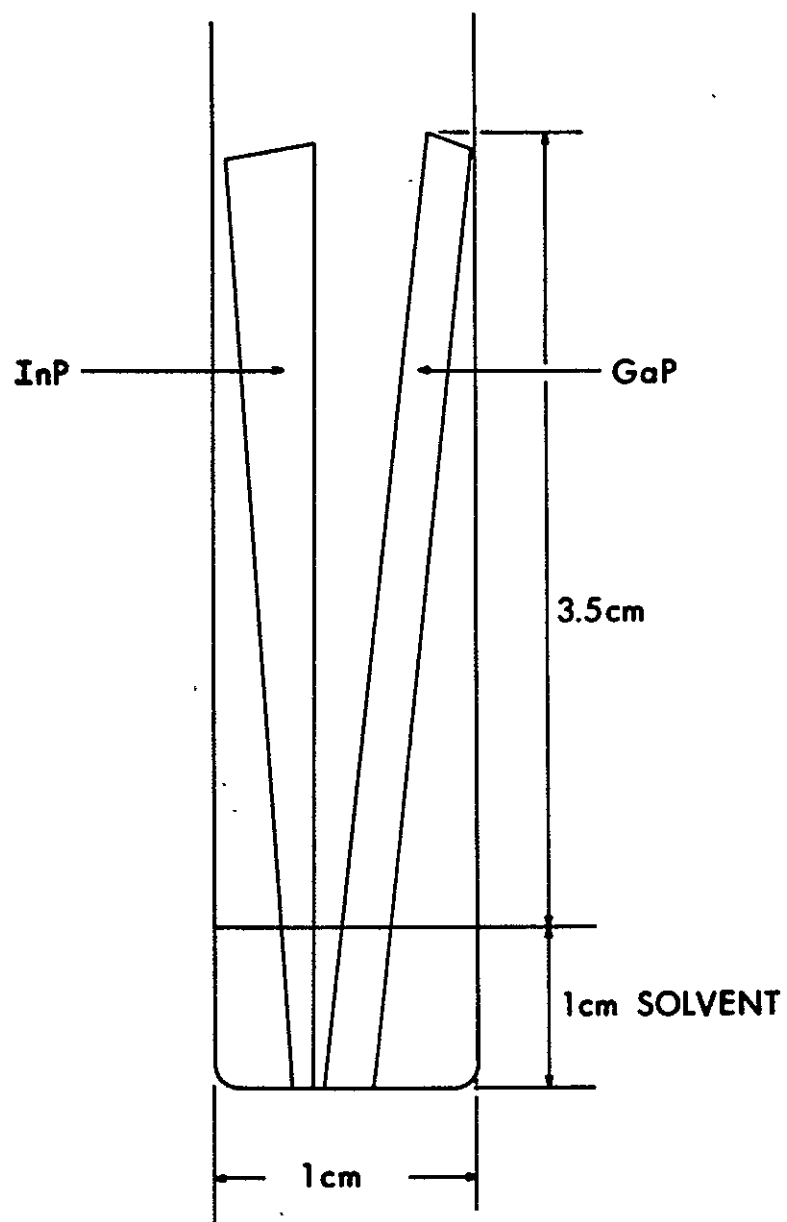


Fig. 10. Schematic illustrating the use of solid rods of GaP and InP as feed material in crystal run #11

constant and composition in (binary) isomorphous systems is linear if there are no volume effects upon mixing. This relationship is "Vegard's rule:"

$$a_x = a_0 (1 + \beta x) \quad (1)$$

Where a_x = lattice parameter of the solid solution crystal of composition $\text{Ga}_x\text{In}_{1-x}\text{P}$

a_0 = lattice parameter of InP

a_1 = lattice parameter of GaP

x = mole fraction of GaP

$$\beta = (a_1 - a_0)/a_0 \quad (2)$$

However, the accuracy of this assumption has been questioned by E-an Zen (Ref. 11) who showed that a second-order correction is necessary if the molar volumes of the end members differ significantly. Zen suggested that it is the molecular volume rather than the lattice parameter that is proportional to composition and that the general relation for the variation of lattice parameter with molar composition in a cubic system is as follows:

$$a_x = a_0 \left\{ 1 - \left[1 - \left(\frac{a_1}{a_0} \right)^3 \right] x \right\}^{1/3} \quad (3)$$

In the case of $\text{Ga}_x\text{In}_{1-x}\text{P}$, where the molar volumes of the end members do differ significantly, this relationship predicts deviations from Vegard's rule of approximately 2% as x approaches 0.5 (see Fig. 11). For greater accuracy in determining composition from lattice parameter, the Zen relationship will be used in this study. Results on the composition of the various samples grown are listed in Table II. For comparison, composition data as derived from optical transmission and electron microprobe analysis are also included in this table.

X-ray analysis: experimental methods. --The Seemann-Bohlin camera (Philips camera no. 52058), which is specifically designed for precision measurement of lattice parameters, has been employed. Unlike the Debye-Scherrer camera which records all 2θ lines, the Seemann-Bohlin (Philips) camera mounts the specimen on the circumference of the camera and records lines for a limited range, $118^\circ < 2\theta \leq 179.48^\circ$. Actual lattice parameter measurements on this Philips camera have shown minimum errors of $\pm 0.0003 \text{ \AA}$ in contrast to the Debye-Scherrer error of $\pm 0.001 \text{ \AA}$. Because of X-ray focusing, this Seemann-Bohlin camera allows for shorter exposure time (Ref. 12).

Other errors such as: (1) eccentricity of sample, (2) radius and shrinkage, and (3) adsorption, are functions of θ and can be eliminated by plotting the lattice parameter measured at each angle versus the Nelson-Riley function

$$1/2 \left(\frac{\cos^2 \theta}{\sin \theta} + \frac{\cos^2 \theta}{\theta} \right) \quad (4)$$

for that angle and extrapolating to the origin by least squares analysis. A representative plot is shown in Fig. 12.

It was mentioned earlier that oxides proved to be detrimental to crystal growth in some of the experiments. An attempt was therefore made to analyze the oxide deposit which had accumulated near the surface of the growing crystal and was suspected to have disrupted its growth.

The X-ray Debye-Scherrer diffraction pattern of the debris collected in experiment no. 12 showed a broad amorphous ring around the low angle hole which effectively masked all

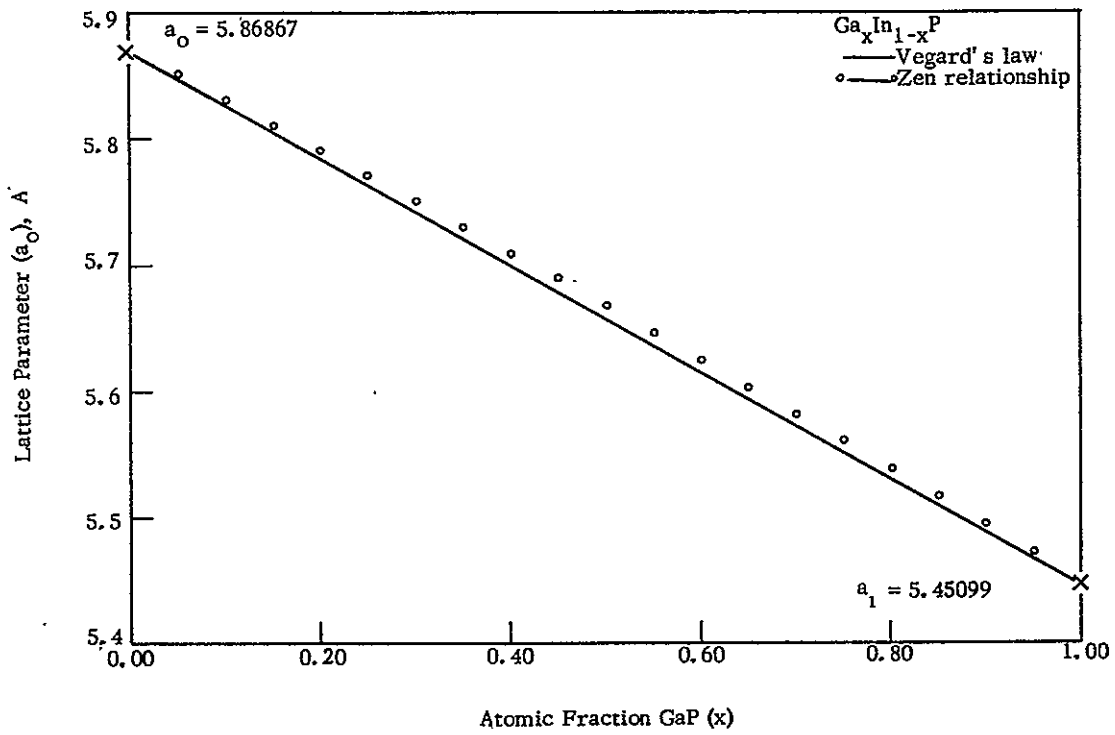


Fig. 11. Variation of lattice parameter with composition illustrating the correction to Vegard's rule introduced by the Zen relationship

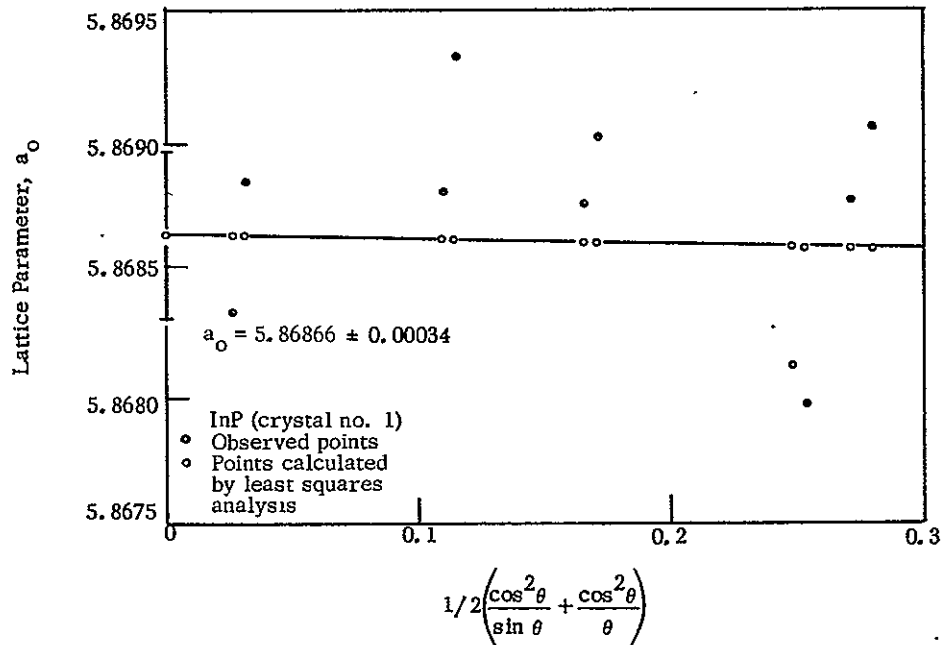


Fig. 12. Calculation of lattice parameter of inhouse InP

Table II. Physical Evaluation of Regrowth Composition of GaP, mol % (=100x)

Run No.	Slice No.	Remarks	By X-Ray	By Optical Adsorption	By Microprobe ^a
1 ^b		Growth affected by two public power failures	8 to 15		
2	3 4 5 (see Fig. 13)		55 ± 1 ^c 68 ± 1 ^d	40 ± 1 ^d 57.8 ± 0.3 ^{c, d, e} 73 ± 1 ^d	65 ^c 90 ^d
10 (see Fig. 14)			37 ± 1	41.0 ± 0.9 ^{e, f}	
18			1 ± 1		
20			1.5 ± 1		
2i	2 3 4 (un-polished) 4 (polished) 5		79 ± 1 79 ± 1 77.5 ± 1 78 ± 1 74 ± 1		
22			80 ± 5 ^e		

- a) Courtesy of Dr. S. Fischler CTM, NASA.
- b) Electrical resistivity 0.1 ohm-cm.
- c) Center section.
- d) Rim section.
- e) Weighted average and error.
- f) Axial slice.

lines corresponding to an interplanar d-spacing greater than 2 \AA . Four diffraction lines were observed ($d_1 = 1.99141 \text{ \AA}$, $d_2 = 1.7247 \text{ \AA}$, $d_3 = 1.23633 \text{ \AA}$, and $d_4 = 1.06674 \text{ \AA}$).

The ratios of the first to second and the third to fourth d-spacings, respectively, corresponded closely to the value $3/2$. Additional probing then showed [from a logarithmic plot of d versus tentative values of $(h^2 + k^2 + l^2)$] that most likely a face-centered cubic or pseudocubic material was present. The lattice constant of this material was 6.9 to 7.0 \AA . A closer check showed the respective structure to be closely related to the tetragonal $\alpha\text{-SiO}_2$ (or low cristobalite SiO_2) structure. SiO_2 of cristobalite structure had been found to form on quartz walls which contact with GaAs melt (Ref. 13). The presence of cristobalite (or perhaps tridymite) is possible but unlikely, however, since the lattice spacing differs too much from ASTM values. It is, therefore, concluded that $(\text{Ga, In})\text{PO}_4$ as such or as a solid solution with SiO_2 has formed.

The noncentrosymmetrical equivalent tetragonal or orthorhombic structure can exist in GaPO_4 and AlPO_4 . In this case, GaPO_4 or $(\text{Ga, In})\text{-PO}_4$ may thus have formed from the oxides present in the metal under the given conditions and contributed to the disruption of growth. The X-ray rules out the presence of $(\text{Ga, In})_2\text{O}_3$ of cubic $\alpha\text{-Mn}_2\text{O}_3$ structure.

In conclusion, there is an oxide and another unknown impurity (causing broad "amorphous" rings in the diffraction pattern). Both of these must be removed from the starting material in order to improve crystal growth.

Equipment and technique for electrical measurements. --Several different techniques are being used for the evaluation of the electrical properties of $\text{Ga}_x\text{In}_{1-x}\text{P}$. Preliminary estimates of the conductivity are made using a so-called contactless probe. The instrument (Triconix, Inc., resistivity meter model NNP) works essentially by measuring the loss of an RF coil which is placed against the surface of the semiconductor; i. e., the lower the resistivity the greater the loading. Measurements of resistivity between 0.005 and 5 ohm-cm are possible using the $1/8$ -in. -diameter coil. The carrier type may be determined by using a hot probe if the resistivity is not too high.

Optical and near infrared measurements. --The most direct method of determining the energy band gap of semiconductors is to measure the optical or infrared absorption edge. The straight dashed lines in Fig. 1 show the energy levels in $\text{Ga}_x\text{In}_{1-x}\text{P}$ which were predicted by using the energy levels determined for the pure end members and by assuming a linear dependence of energy levels on concentration. However, Lorenz, et al. (Ref. 15), have measured the energy band gap as a function of composition. The results, replotted in Fig. 1 solid lines, differ greatly from the assumed linear dependence. $\text{Ga}_x\text{In}_{1-x}\text{P}$ has a direct band gap ($\Gamma_1 - \Gamma_{15}$) for $0 \leq x \leq 0.8$. The largest direct gap is 2.2 eV corresponding to a wavelength of 5600 \AA .

Optical transmission measurements have been made on several samples of $\text{Ga}_x\text{In}_{1-x}\text{P}$ to determine their bandwidth. Some typical results are shown in Fig. 13 for run no. 2, slice 5, where the energy gap was determined at a number of different positions. A mask was positioned over the sample so that transmission was restricted to an area approximately 2 by 2 mm . Also shown in Fig. 13 are the estimated compositions which were obtained by using the results of Lorenz, et al. (Ref. 1), for the energy band gap as a function of composition in Fig. 1.

In run no. 2, there is some variation of the composition within one slice as well as a composition gradient from slice to slice. The initial composition at the start of the growth

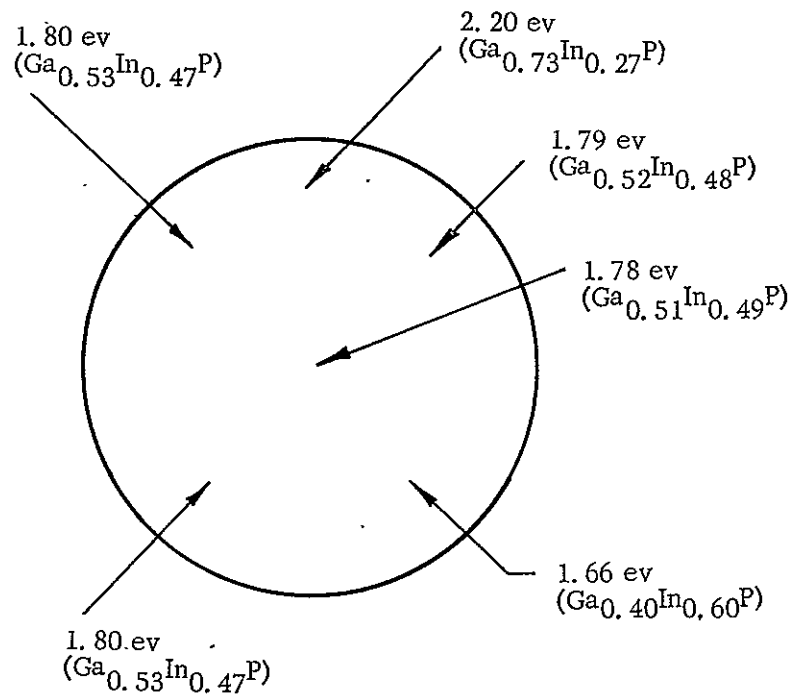


Fig. 13. Band gap energy as determined by optical transmission at various positions for slice no. 5, run no. 2 (composition determined using data of Lorenz, et al. 1)

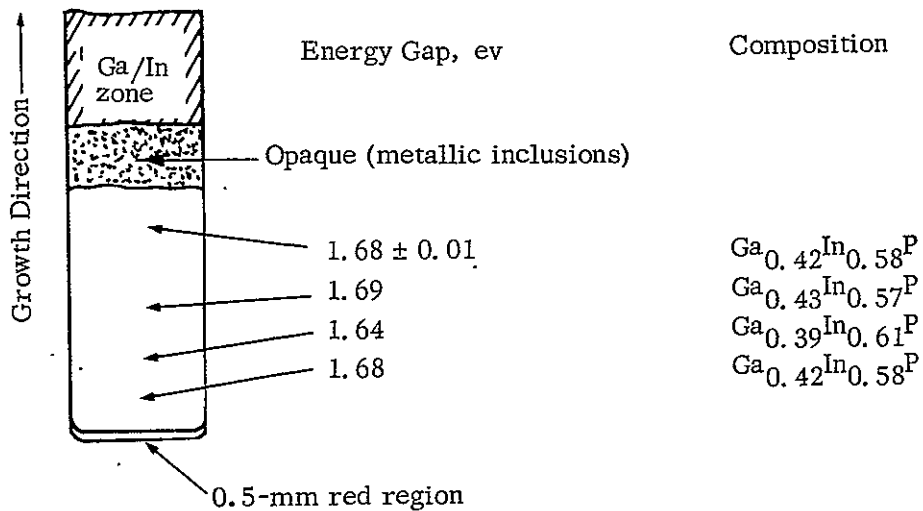


Fig. 14. Energy gap of Ga_xIn_{1-x}P, run no. 10 (shown in Fig. 6) determined by optical transmission along growth direction (also shown in composition estimated from work of Lorenz, et al. Ref. 1)

was high in GaP, but as the growth progressed, the GaP/InP ration approached that of the feed material.

A slice parallel to the growth direction was cut from run no. 10, and optical measurements were made as a function of its position along the growth axis. Fig. 14 shows the results of these measurements. Except for approximately a 0.5-cm region at the start of growth, the material is relatively uniform both parallel and perpendicular to the growth direction.

Comparison of optical and X-ray data obtained on $Ga_xIn_{1-x}P$: -- Selected results obtained from electrical, optical, and X-ray measurements as reported in the preceding sections are shown in Table II. Where comparisons between X-ray and optical absorption data can be made, results agree to a first approximation. Composition obtained in the grown material was generally in the desirable concentration range when the produced crystals were of sufficient length. Their GaP content was often found to be low, however (as in experiments 18 and 20), when growth was short or interrupted.

From Figs. 13, 14 and Table II, it appears that the compositional homogeneity of the solid solution material grown by THM can be quite good as in samples nos. 2, 10 and 21. It is to be noted, however, that slices nos. 1 through 4 of the early sample no. 2 contained distinctly opaque and transparent sections. A similar observation had been made earlier when overgrowth of InP-rich single crystals of 35 mol % GaP on GaP-rich crystals of 65 mol % GaP occurred during cooling from $In_{0.9}Ga_{0.1}$ solvent (Ref. 5). Since there is obviously no miscibility gap in the GaP-InP system (Ref. 14), the phenomenon can alternately be explained as discussed below.

Within a given range of liquidus-solidus composition, only a small change in the liquidus composition is associated with a large change in solidus composition. This phase relation in turn could cause the rate and/or free energy of the epitaxial nucleation of the InP-rich phase on the GaP-rich phase to surpass the rate and/or free energy of continued growth on the GaP-rich phase.

A weighted error analysis was made of sample no. 2, slice no. 5 (Fig. 13) and sample no. 10 (Fig. 14). It showed that, within the error confidence limits (for which one-third of the maximum difference between a given value and the weighted average is less than their weighted error), sample no. 10 proved to be uniform; sample no. 2, slice no. 5 also proved uniform except for the two regions exhibiting optical energy gaps of 1.66 eV and 2.20 eV, respectively.

Since distinctly opaque and transparent section were observed only occasionally, it is concluded that the rate of heater movement is sufficiently slow. Nevertheless, a somewhat slower rate of movement of perhaps 2 mm/day may more safely prevent the reoccurrence of the secondary off-equilibrium nucleation and heterogeneous epitaxy of the InP rich phase. It will also be helpful to increase the solution zone temperature and consequently the solid-liquid temperature. This will render the ratio of solidus to liquidus composition ratio less sensitive to small temperature changes. Both measures (i. e., zone temperature increase and lowering of growth rate or heater movement) will effectively prevent the simultaneous formation of opaque and transparent secondary "phase regions."

CONCLUSIONS AND RECOMMENDATIONS

In the THM growth of $\text{Ga}_x\text{In}_{1-x}\text{P}$, a charge of feed and seed crystal separated by a solvent zone is sealed in a quartz tube and slowly lowered through a vertical hot zone furnace as shown in Fig. 4. The molten zone is thus made to move through the feed material in this way causing a crystal of the desired composition to deposit on the seed.

The crystal growth rate is controlled by the diffusion of atomic or molecular species across the solution zone. As a consequence, the rate of movement of the charge relative to the hot zone of the furnace must not exceed 4 mm/day, but should preferably be as low as 2 mm/day.

The growth of $\text{Ga}_x\text{In}_{1-x}\text{P}$ of uniform composition by THM can best be achieved when the following conditions (relative to feed material, solution zone, and temperature) are met: (1) feed material should be a solid ingot of uniform composition, (2) for a given growth rate and temperature, the length and the composition $\text{Ga}_y\text{In}_z\text{P}_{1-y-z}$ of the molten solution zone must be chosen so as to remain unchanged during growth, and (3) the temperature at all points within the moving zone and the adjacent feed ingot and growing ingot must also remain unchanged during growth. Under these conditions, the composition of the depositing growth will be the same as the feed at all times, i. e., from the start of the growth until the moment the feed is consumed.

It is normally not possible to satisfy all three conditions at once. First, if uniform $\text{Ga}_x\text{In}_{1-x}\text{P}$ ingots of sufficient quality could be made available by some other method, then their production by THM would not be necessary. Rapid freezing of a molten mixture of GaP-InP would be a possible method for the preparation of solid ingots of fair average axial homogeneity. However, the phosphorus decomposition pressure over material of the required GaP content at its freezing point is unfortunately too high to make this approach feasible. Second, and third, although the effect of growth rate (if less than 3 mm/day) can be neglected, and the liquidus composition (if known from the phase diagram) could be chosen for the solution zone, a number of exploratory tests would still be required to achieve a given steady state temperature and temperature field in the growth experiments. It is therefore practical to choose tentatively some estimated values of zone length (e. g., 1 to 1.5 cm), solvent composition (e. g. $\text{Ga}_{0.35}\text{In}_{0.65}$) and zone temperature (e. g., 1100 °C would be preferred) for the experimental conditions. During the early phase of the growth runs thus conducted, these parameters will approach constant, steady state values in time. Often, steady state may be attained after a short initial growth of approximately 3 to 5 mm. Conditions (2) and (3) can thus be satisfied without great difficulties. Relating to point (1), it is suggested that solid, non-porous ingots be first grown as "first preparations," to be used later as feed material for the growth of truly homogeneous "second preparations." In addition, the temperature of the interface of the growing crystal (in contact with the liquid zone) should be increased to about 1100 °C to improve further the compositional homogeneity of the resulting material.

A single step effort was made to increase the GaP mole fraction x from 0.63 to 0.75. The fact that this attempt proved successful shows that the careful appraisal and application of phase relations may often be preferable to empirical adjustments even in difficult ternary systems, in particular, when expense and time are determining factors in the experiments.

REFERENCES

1. Lorenz, M. R., Reuter, W., Dumke, W. P., Chicotka, R. J., Pettit, G. D., and Woodall, J. M., Band Structure and Direct Transition Electroluminescence in the $\text{In}_{1-x}\text{Ga}_x\text{P}$ Alloys, *Appl. Phys. Letters*, 13, (1969), p. 421.
2. Saul, R. H., Armstrong, J., and Hackett, Jr., W. H. : GaP Red Electroluminescent Diodes With an External Quantum Efficiency of 7%. *Appl. Phys. Letters*, 15, 1969, p. 229.
3. Pilkuhn, M. and Rupprecht, H. : Electroluminescence and Lasing Action in $\text{GaAs}_x\text{P}_{1-x}$. *J. Appl. Phys.*, 36, 1965, p. 684.
4. Wolff, G. A., Hebert, R. A., and Broder, J. D. : Electroluminescence of GaP. *Phys. Rev.*, 100, 1955, p. 1144.
5. Wolff, G. A., Hebert, R. A., and Broder, J. D. : Recent Investigations on the Electroluminescence of GaP. *Proc. Intern. Conf. on Semiconductors and Phosphors*, 1958, p. 547.
6. Hilsun, C. : Some Key Features of III-V Compounds. *Semiconductors and Semimetals, Vol. 1: Physics of III-V Compounds*. R. K. Willardson and A. C. Beer, eds., New York, Academic Press, 1966.
7. Wolff, G. A. and Mlavsky, A. I. : The Growth of Crystals by Solvent Zone Techniques—A Review. *Proc. Intern. Conf. on Adsorption and Crystal Growth*, Nancy, France Centre National de la Recherche Scientifique, Paris, France, Publication No. 152, 1965, p. 339; p. 711.
8. Wolff, G. A., LaBelle, Jr., H. E., and Das, B. N. : Solution Growth of (Zn,Hg)Te and Ga(P,As) Crystals. *Trans. TMS-AIME*, 242, 1968, p. 436.
9. Broder, J. D. and Wolff, G. A. : A New Method of GaP Growth. *J. Electrochem. Soc.*, 110, 1963, p. 1150.
10. Panish, M. B. and Arthur, J. R. : The Ga-In-P System. *J. Chem. Thermodynamics*, 2, 1970, p. 319.
11. Zen, E-an: Validity of Vegard's Law. *Amer. Mineralogist*, 41, 1956, p. 523.
12. Taylor, A. : X-Ray Metallography. John Wiley and Sons, Inc., N. Y., 1961.
13. Yamaguchi, M., Mizushima, Y., Hirota, S., and Noake, H. : Cristobalite Formation on Vitreous Silica Boats and the Relation to the GaAs Crystal Growing. *J. Electrochem. Soc.*, 113, 1966, p. 294.
14. Foster, L. M. and Scardefield, J. E. : The Solidus Boundary in the GaP-InP Pseudo-binary System. *J. Electrochem. Soc.*, 117, 1970, p. 534.

Appendix A

SOLUTION GROWTH OF ELECTRONIC COMPOUNDS AND THEIR SOLID SOLUTIONS

N. Hemmat, C. B. Lamport, A. A. Menna, and G. A. Wolff

This paper has been presented at the 67th national meeting of the American Institute of Chemical Engineers in Atlanta, Georgia, on August 16, 1970, and published in the Conference Proceedings "Preprint Volume Materials Engineering and Sciences Division Biennial Conference," February 15-18, 1970, pp. 112-121.

ABSTRACT

The growth of crystals from solution is generally diffusion controlled and slower than growth from either melt or vapor. For this reason, compositional variations in the depositing material due to temperature fluctuations are greatly decreased. Microhomogeneity is especially important in solid solutions or doped compounds. Macroscopic homogeneity can be achieved by steady state growth conditions, as in the travelling heater method. In this method, a liquid solvent zone is moved through the solid feed material by means of a heater, and constitutional supercooling is avoided by heating the center of the solution zone beyond a critical peak temperature.

INTRODUCTION

Crystal growth from solution has been proved to have certain advantages. For example, peritectic materials can be readily grown by this method.

It is also advantageous in the growth of other compounds (such as cubic CuCl) in which phase transformation occurs upon heating. Crystals generally grow much more slowly from solution than from either their melt or vapor phase. For a crystal to grow from solution, its molecular species must diffuse through the solution to the crystal surface. Since, in general, diffusion in the liquid is slow, then the rate of crystal growth from solution is also slow. In this type of growth, however, the detrimental effect of temperature fluctuations on crystal homogeneity is much less severe than in melt or vapor growth. When crystals are grown by slow cooling from solution, the crystal seed formation and growth are governed by the occurrence of statistical events and do not follow a controlled pattern.

In another type of solution growth, namely, the "travelling solvent method" (TSM), a "thin" solvent zone moves under the influence of a temperature gradient through the material, thus producing crystals at the receding end of the liquid zone. This technique is best applied for the growth of thin crystals and p-n junctions in semiconductor materials (1, 2).

For the growth of large single crystals, another variation of solution growth, called the "travelling heater method" (THM), has been applied (3). In this technique, a "thick" solvent zone is used and the driving force for solution zone movement is provided by a travelling heater. This crystal growth method will be the main subject of this article, with emphasis on its application to electronic materials.

Page 26 Missing in
Original Document

p 26 missing
in original

CONVENTIONAL CRYSTAL GROWTH TECHNIQUES

The conventional techniques applied in crystal growth can be divided into four main categories:

1. Growth from the melt either by directional solidification of the melt (as in the Bridgman, Czochralski, and Verneuil techniques), or by moving a molten zone through a solid feed material by means of an electrical resistance or RF heater. The latter may be achieved with a confining container (zone melting in a horizontal boat) or without one (vertical floating zone melting).

2. Vapor phase growth in which crystals may be produced by either evaporation and condensation or by chemical reaction from the vapor phase, i. e. , by synthesis and subsequent condensation in a closed system or in an open flow system using inert or reducing gases as transport agents. Epitaxial growth from the gaseous phase could also be included in this category (4).

3. Crystallization from solution by slow cooling or evaporation of the solvent. This includes growth from solution at elevated temperature and pressure (hydrothermal growth)*; and epitaxial growth from liquid solutions ("liquid epitaxy") (6).

4. Growth from aqueous solution via chemical reaction where the precipitated nuclei, resulting from chemical dissociation and/or reaction, initiate crystal growth (7). In this type of crystal growth, the rate of reaction and subsequent growth are depressed by the use of gels, or a resting solvent zone, which act as separating and simultaneously as diffusion limiting transport media between two chemical reagents. †

To date, a considerable number of electronic elements, compounds, and their solid solutions have been grown by these techniques on a laboratory or production scale. Strictly speaking, most of them have been grown for use in semiconductor devices (such as diodes of various kinds, transistors, and others); however, a new group of electronic materials have increasingly come into use for devices that utilize electronic phenomena in conjunction with other physical effects. Electroacoustic, galvanomagnetic, lasing, and optoelectronic materials are appropriate examples. Often, when the device in question calls for a single crystal material in the form of a thin film or even a whisker, modification of one or the other of the previously mentioned methods of crystal growth can generally produce the desired single crystal shape.

There are many electronic materials, however, which cannot be made into single crystals of suitable quality by one of the cited techniques and there are others which cannot be obtained at all in single crystal form by these methods. This is true particularly in those cases in which the melting point or the vapor pressure of a singular compound, or of a constituent compound as part of a solid solution, is excessively high. For compounds having high melting points, temperature fluctuations easily cause nonuniform growth from the melt resulting in compositional and stoichiometric inhomogeneity and a high dislocation content in the crystal.

*For details on the various established methods of crystal growth listed here, consult reference (5).

†Although this method has been applied for at least half a century, the use of gels as diffusion and convection limiting media is new.

On the other hand, when the vapor pressure is high, additional nonuniform deposition via the vapor phase may take place due to temperature differences on the surface of the growing crystal. Crystallization from the vapor phase can also suffer from similar shortcomings caused by transient and local temperature fluctuations which frequently result in crystal twinning, stacking faults, and related heterogeneities and inhomogeneities. Since crystal growth from the vapor phase is normally catalyzed by dislocations, the latter will generally propagate or even increase in number. In addition, special problems of a technical or engineering nature arise in dealing with high melting and high pressure materials: special designs of apparatus are necessary, and precautions in experimentation must be taken in order to prevent explosions, for instance.

Solution growth, particularly by slow cooling, does not pose the same types of problems. The liquidus (crystallization) temperature can be chosen much below the melting temperature of the material, and the vapor pressure is often greatly decreased if the proper solvent material is chosen. The growth of GaP from liquid gallium solvent is a pertinent example (8). This type of growth has the advantage that the crystal can be grown constraint free.

The disadvantage is, however, that two-dimensional nucleation or dislocation catalyzed growth is promoted and preferred on crystal extremities, such as on crystal edges and apices. Thus "crystal hopper" growth occurs or accidental protrusions form at the crystal surface resulting in dendritic or cellular growth because of the presence of constitutional supercooling. The basic reason for this is a perturbed diffusion potential and solute concentration profile in the solution next to the growing crystal. Solvent inclusions and other crystal inhomogeneities may also result from these effects.

In the light of the preceding remarks, and from the description of the "travelling heater method" (THM) which will follow, the choice of this method for the growth of a large variety of compounds and their solid solutions in preference to other methods can be understood. In THM, the crystal growth rate is also controlled and limited by the diffusion rate of solute in the solution, as is the case in regular solution growth by slow cooling. The growth rate can be monitored, however, in such a way that constitutional supercooling and solvent inclusions can be avoided (9, 10). As in normal solution growth or in TSM (3, 11, 12), the dislocation content obtained in THM grown crystals remains low. The fact that crystals of peritectically melting materials have been prepared in this way also demonstrates the general applicability of this method (13).

CRYSTAL GROWTH BY THE TRAVELLING HEATER METHOD

General

The travelling heater method of crystal growth refers to the technique in which a molten solvent zone is made to move through a solid source material by the slow movement of the charge material relative to the solution zone heater, or vice versa. In this process, the dissolution of feed material occurs at the receding (liquid) solid interface, and the crystallization of the dissolved feed occurs at the advancing (liquid) solid interface. Figs. A-1 and A-2 show respectively, schematics of the mechanism and apparatus for crystal growth by THM.

A simplified theoretical analysis of crystal growth by THM has been published previously (3, 9, 14). Some of the important points may be summarized as follows. The growth rate is determined by the highest possible diffusion rate of the most slowly diffusing constituent species through the solution zone. In general, the critical growth rate limit is less than

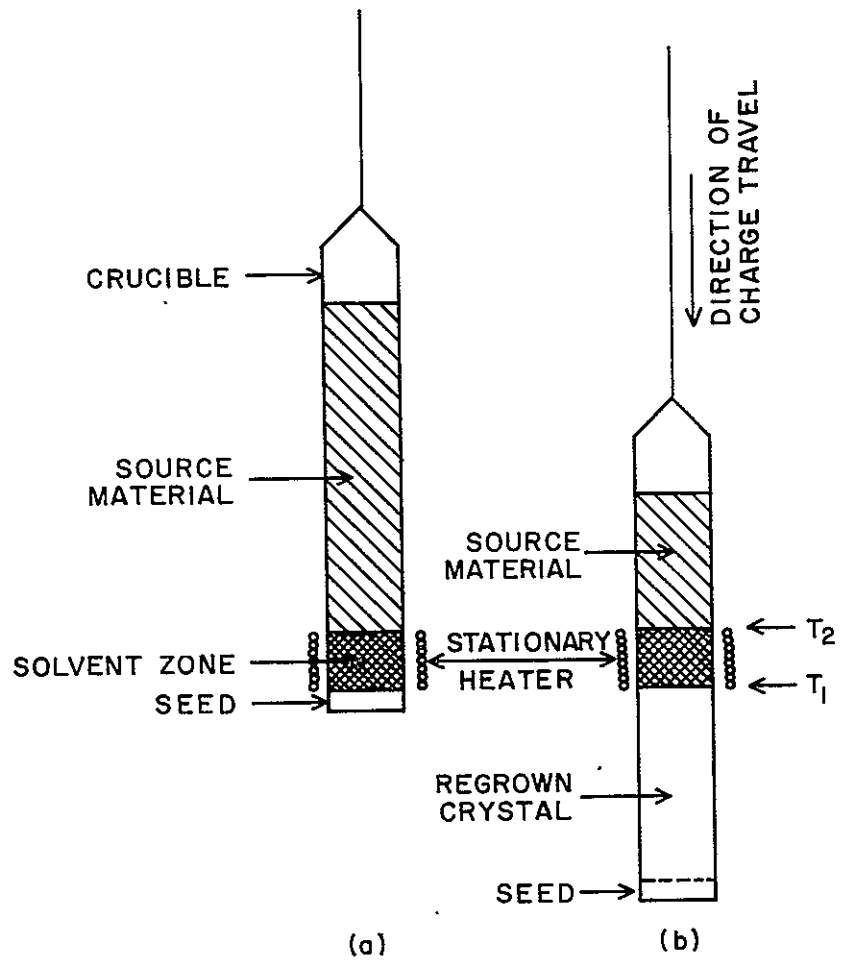


Fig. A-1. Schematic of zone movement process in travelling heater method (THM)

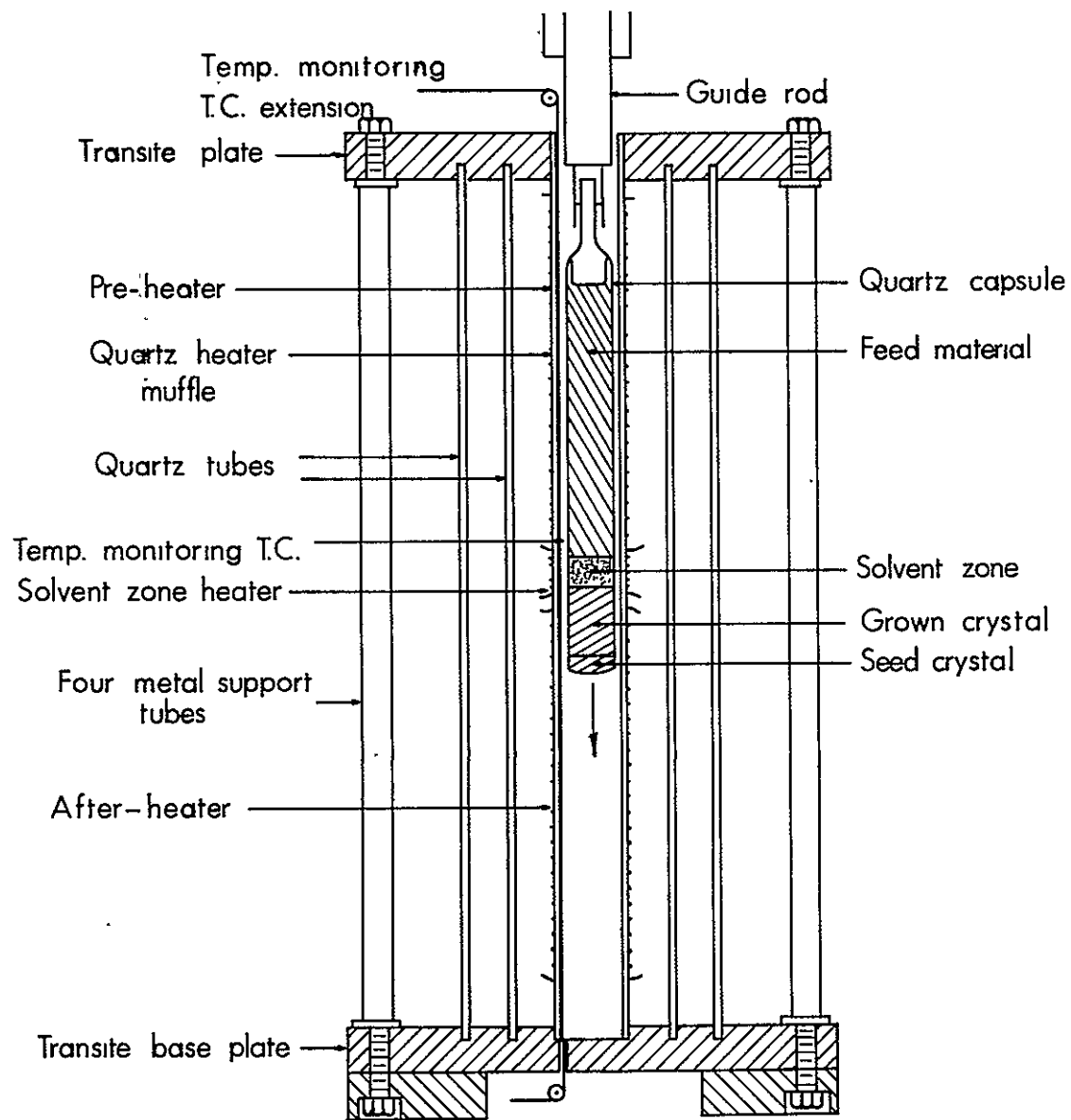


Fig. A-2. Apparatus for crystal growth by travelling heater method

6 mm/day. High solvent viscosity or an anomalously low diffusion coefficient may further depress this value to 1 mm/day.

The critical maximum growth rate equals the product of the diffusion constant of the slowly diffusing solution species in the liquid times its (negative) concentration gradient across the solution zone. In order to achieve a reasonable growth rate, the mean solution zone temperature must be high enough to ensure a sufficiently high solubility of the feed material in the solvent

An estimate of the minimum mean interface temperature $(T' + T'')/2$, where T' and T'' are, respectively, the temperatures of growing and dissolving solid (liquid) interfaces at which crystal growth becomes fast enough for practical purposes can be obtained from the solvent-solute phase diagram. For the chosen composition of the solid to be grown, that liquidus temperature at which the solid is in equilibrium with its solution and at which the concentration of the most slowly diffusing species is still sufficiently high in the liquid solution, say, perhaps 2 mole percent, is chosen. In the case of solid solutions that can be considered part of a ternary phase diagram, this procedure in fact corresponds to selecting the appropriate tieline terminating at either end of the liquidus and solidus surfaces of the phase diagram at points of the above mentioned compositions of liquid and solid. The point on the liquidus surface then yields the required mean minimum interface temperature at which crystal growth operation becomes feasible. A practical example may be given. For the THM growth of $Al_{0.1}Ga_{0.9}As$ from an Al-Ga solvent, a solution zone temperature in excess of 1000 °C is necessary. This can be deduced from the Al-Ga-As phase diagram section given in Fig. A-3 (see also Fig. A-4 for most detail). A slice of the resulting material is shown in Fig. A-5.

Another advantage of THM is the bulk crystal growth of materials which melt peritectically (i. e. , decompose into a liquid and solid, both of which differ in composition with respect to the peritectic material), or of materials that at the melting point evaporate incongruently and require relatively high pressures to prevent their dissociation. Solid solutions are another group of materials to be mentioned in this context.

Other advantages are: (1) highly reactive materials can be grown at a temperature considerably below their melting point, (2) single crystal seeding can be applied, and (3) crystals of increased perfection can be grown. As in zone melting, purification of the source material results from passing the solvent zone through the source material.

Selection of a suitable solvent for crystal growth by THM not only depends on the particular class of material (i. e. , element, compound, solid solution) to be processed, but is also related to the metallurgical and electronic properties of the source material. A suitably selected solvent should possess the following favorable properties:

1. A sufficiently high solubility in the liquid state for the material in question at moderate temperatures
2. A negligible solubility in the solid to be grown
3. No compound formation with either the material to be grown or with any one of its constituent elements
4. Low vapor pressure at growth temperatures
5. Good wetting properties with feed and seed material
6. A segregation coefficient less than unity for the impurities generally present in the source material

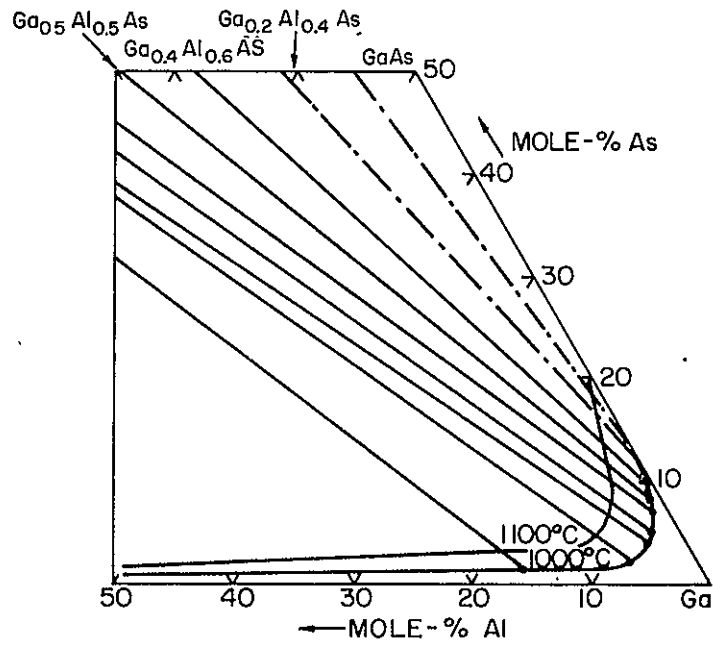


Fig. A-3. Section of Ga-Al-As phase diagram as derived from reference 15

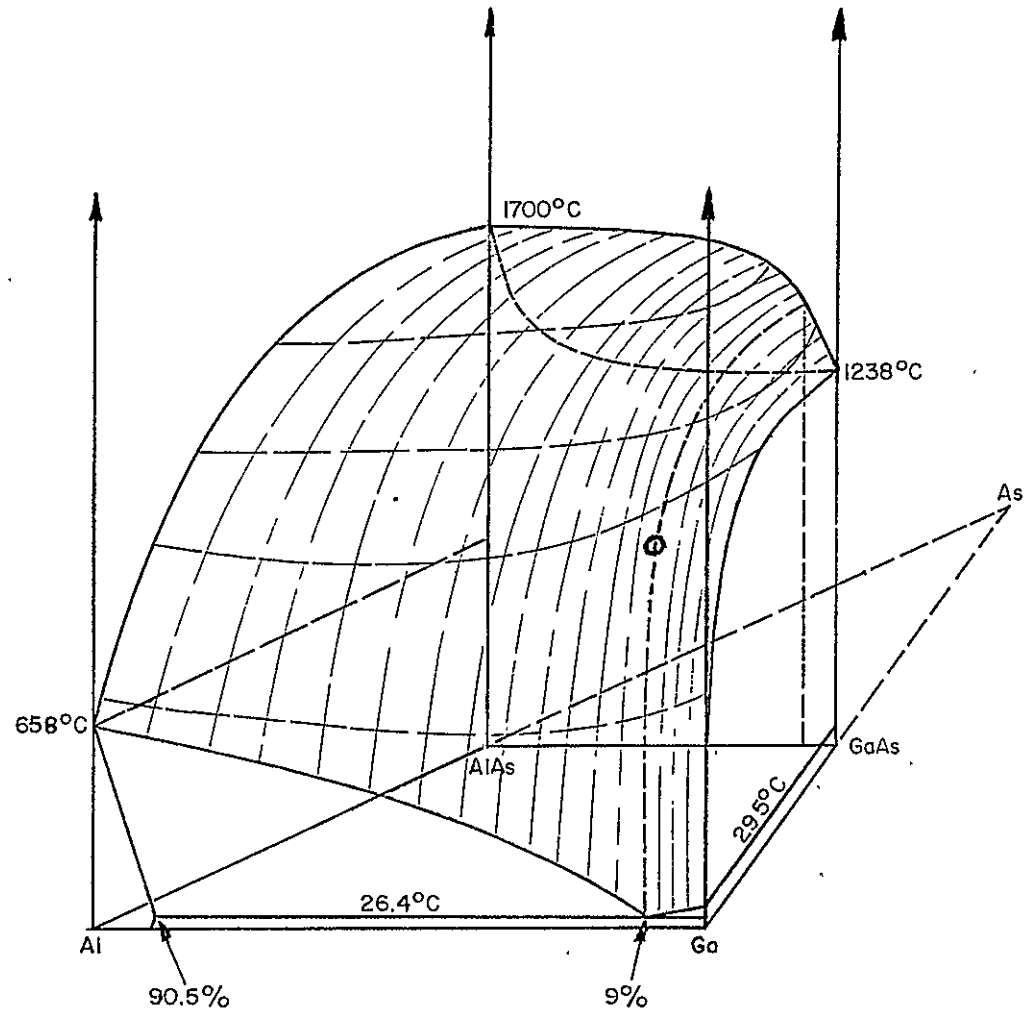


Fig. A-4. T, x phase diagram of Ga-As-Al-As-Al-Ga system (circled position on liquidus surface indicates suggested growth conditions)

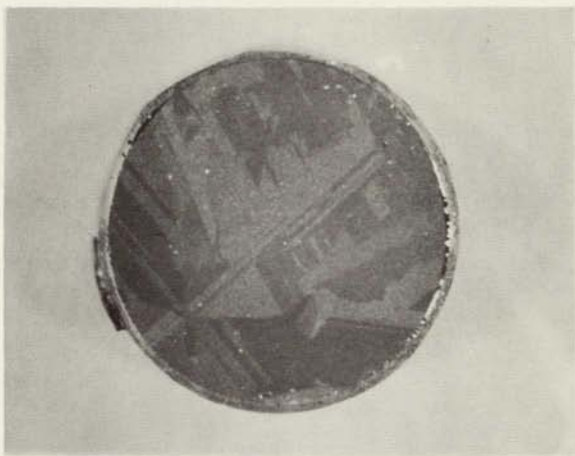


Fig. A-5. Slice from $\text{Al}_{1.1}\text{Ga}_{0.9}\text{As}$ ingot grown by THM from feed mixture of AlAs and GaAs using $\text{Al}_{0.03}\text{Ga}_{0.97}$ as starting composition of solvent

7. No reaction with the container material at crystal growth temperatures
 8. No detrimental electronic (doping) effects on the material to be grown
 9. Where electronic doping from the solvent is desirable, however, the solvent should be chosen accordingly. Here, stoichiometric control is particularly useful, as in the growth of GaSb from its molten solution in either Ga or Sb, or of $Zn_xHg_{1-x}Te$ from its solution in molten Te, for instance. Decrease of the growth temperature in general increases effects of doping due to either impurities or intrinsic deviations from stoichiometry.

In this method, it is imperative that there be no constitutional supercooling within the solution zone next to either one of the liquid-solid boundaries, i. e. , within the regions adjacent to the growing and dissolving crystal. It is therefore necessary that the center of the solution zone be heated to a peak temperature by the zone heater so that the temperature gradient (towards the solid) at either interface is less than the respective gradient corresponding to the equilibrium temperature.

In a relative sense, thermal conduction and temperature gradients are generally less sensitive to monitoring by means of a heat source or heat sink control than are diffusion rates and concentration gradients. Thermal conduction parameters, therefore, largely dictate experimental conditions and design. If the thermal conductivity of the solution zone is relatively large, then the zone length must also be increased so that towards either end, i. e. , seed and feed, the magnitude of its (negative) temperature gradient is sufficient to prevent constitutional supercooling.

Heat and material transport can generally be expressed by means of the equation:

$$D \nabla^2 V = \frac{\partial V}{\partial t} \quad (A-1)$$

where D and V represent, respectively, the thermal conductivity and temperature (for heat transport), or material diffusivity and concentration (for material transport). Since steady state conditions prevail, Eq. (A-1) becomes zero. Expressed in cylindrical coordinates, Eq. (A-1) becomes:

$$\frac{\partial^2 V}{\partial r^2} + \frac{1}{r} \frac{\partial V}{\partial r} + \frac{\partial^2 V}{\partial z^2} + \frac{1}{r^2} \frac{\partial^2 V}{\partial \phi^2} = 0 \quad (A-2)$$

where, because of rotational symmetry, the last term vanishes.

With the boundary condition:

$$\frac{\partial V}{\partial r} (r=0, z) = 0 \quad (A-3)$$

the general solution

$$V = \sum_k C_{1k} J_0(kr) [C_{2k} \cosh(kz) + C_{3k} \sinh(kz)] \quad (A-4)$$

results. Here, $J_0(kr)$ is the Bessel function of the first kind of zero order and k is a parameter which need not be an integer.

Space prohibits a detailed discussion of the effect of the various boundary conditions on this solution. It should be mentioned, however, that the solutions for thermal and material transport will be basically different. For simultaneous, independent (material) transport of two different species of concentrations A and B , a diffusion potential for constant A/B ratio can be derived. This can give rise to a radial composition gradient in the material grown. Apparently, the asymmetrical terms, $C_3 k \sinh(kz)$, are also functions of the growth rate. Although various particular solutions for temperature and concentration distribution have been given for related crystal growth systems, this particular system has not as yet been analyzed sufficiently.

Application and Discussion

The basic principle of THM growth was first suggested by Hein in a patent disclosure on the preparation of pure crystalline silicon (16). In this patent, the passage of a zone of molten Au-Si alloy through silicon is proposed for its purification, using RF heating and a travelling rate of 40 to 2000 cm/day. Mason and Cook (13) have applied this method to the growth of peritectic compounds as suggested first by Goodman (17). With a travelling rate of 3 to 20 cm/day, they obtained $CdIn_2Te_4$ polycrystals of good uniformity which in some cases contained small second phase particles at grain boundaries. Single crystals of yttrium iron garnet (YIG) were obtained by a floating zone technique at rates of 3 to 5 cm/day (18). A modification of this crystal growth technique, using a linear temperature gradient across the solution zone, was proposed by Pfann (19).

TABLE A-1
EXPERIMENTAL DATA ON MATERIALS GROWN BY THM OR RELATED METHODS

Solvent	Material	Growth Rate, mm/day	Heater	Reference
In_2Te_3 -CdTe	$CdIn_2Te_4$	30 to 200	RH	(13)
Fe_2O_3 -YFeO ₃	YIG	30 to 150	RF	(18)
Au-Si	Si	0.4 to 20m	RF	(16)
Cr	SiC	≤ 3	RF	(10)
Ga	GaP	4	RF	(20)
Ga	GaP, Ga(As, P)	≤ 5 to 6	RF	(9, 14)
Ga-In	(Ga, In)P	≤ 3 to 5	RH	(21)
Al-Ga	(Al, Ga)As	≤ 3 to 5	RH	(21)
Ga	GaAs	≤ 5	RH	(21)
Te	HgTe, ZnTe (Hg, Zn)Te	≤ 3 to 5	RH	(9)
Te	CdTe	≤ 5 to 7.5	RH	(22)
PbF_2	ZnO	≤ 3	RF	(23)
KCl	CuCl	5 to 6	RH	(24)
(Ba, Sr)Cl ₂				
CdCl ₂	$CdCr_2Se_4$	≤ 1.5	RH	(21)
Borate	(Pb, Sr)TiO ₃	≤ 1	RF	(25)
Flux	Pb(Ti, Zr)O ₃	≤ 1	RF	(25)

Table A-1 lists materials previously grown by THM or variants of this method. This table also includes experimental data specifying the solvent employed, the maximum or applied growth rate, the mode of heating [i. e. , resistance heating (RH) or RF heating] as well as references.

The existence of a critical maximum rate above which good crystals cannot be grown is particularly revealing. The critical growth rate directly coincides with the onset of constitutional supercooling in the solution zone. In THM, as in any other type of crystal growth, the exclusion of the solvent or impurities from the growing crystal is equivalent to the prevention of constitutional supercooling. The latter occurs when the value of supersaturation, $c_2/c_{2e} - 1 > 0$, in the solution increases with increasing distance from the growing crystal. Here, c_{2e} and c_2 are, respectively, the equilibrium solute concentration (solubility) and actual solute concentration in the solution. In the following calculations, an axial reference coordinate system z is used instead of the fixed coordinate $x = z + Rt$ (where $z = 0$ at the moving interface of the growing crystal).

If THM growth is diffusion controlled then, for steady state, the growth rate is given by

$$\frac{dx}{dt} = R = \frac{D}{c_1} \frac{dc_2}{dz} = \frac{k_{21}}{c_1} (c_2 - c_{2e}) = \text{constant} \quad (\text{A-5})$$

where c_1 is the molecular concentration per crystal volume and k_{21} is the rate constant governing transfer of solute from solution to solid.

As mentioned before, the absence of constitutional supercooling requires that

$$\frac{d(c_2 - c_{2e})}{dz} = \frac{dc_2}{dz} - \frac{dc_{2e}}{dT} \frac{dT}{dz} \leq 0 \quad (\text{A-6})$$

if k_{21} and D are independent of temperature, T .

Setting $dT/dz \equiv G$, $dT/dc_{2e} \equiv m = \text{slope of liquidus line}$, $c_{2e} \approx B \exp(-\lambda/RT)$, Eq. (A-6) can be rearranged as follows:

$$\frac{G}{R} \geq \frac{c_1 m}{D} \approx \frac{c_1 k T^2}{D \lambda c_{2e}} \quad (\text{A-7})$$

for low solute solubility, no solid solubility of solvent in the crystal, and the absence of constitutional supercooling. The ratio G_c/R_c of the critical temperature gradient (across the solution zone) and critical growth rate are obtained by equating the first two terms of Eq. (A-7).

In the special case of THM growth, this expression is thus similar to Eq. (A-8) which has been derived by Tiller, et al. (26):

$$\frac{G_c}{R_c} = \frac{m c_1 (1 - k)}{kD} \quad (\text{A-8})$$

where k is the distribution coefficient.

There is still another critical situation in THM growth that occurs when the movement of the advancing crystal growth front lags with respect to the rate of the heater movement. Short periods of sporadic crystal growth then alternate with periods of retention of massive amounts of solvent. According to Eq. (A-5), the onset of this discontinuation of growth should occur when the rate of heater movement exceeds the maximum growth rate (R) which can still be accommodated by the rate of diffusion of solute in the solution.

With the preceding outline in mind, it is now appropriate to examine the observed critical growth rates and experimental growth rate values shown in Table A-I. All critical growth rate values of growth rates are within the range 1 to 7.5 mm/day. This is surprising, since the materials in question vary widely in properties such as thermal conductivity, solubility in solvent, etc., and also the solvent and growth temperature applied differ just as much. It can only be conjectured that in these cases a number of factors of opposite trend compensate each other. One might tentatively conclude, however, that the lowest values of the critical growth rates, R_c , in Table I are caused by a high viscosity rather than low thermal conductivity as in Borate flux and in molten CdCl_2 .

These values shown in Table A-I compare favorably with R values observed for TSM grown materials. The following values (in mm/day) have been measured in TSM growth:

GaAs from Ga: 12(1)

GaP from Ga: 12(27)

SiC from Cr: 3(2)

In the growth of binary solid solution alloys from their melt by zone leveling, the growth rates are also comparable with the values observed in THM, i. e., for alloys near the 1:1 alloy composition. At this composition, the liquidus-solidus separation becomes widest and diffusion control of crystal growth thus becomes prominent. The values (in mm/day) are as follows:

$\text{Ge}_{0.55}\text{Si}_{0.45}$ from molten alloy: 26 (28)

$\text{Bi}_{0.4}\text{Sb}_{0.6}$ from molten alloy: 5.2 (29)

From this point of view, the growth rates of 40 to 2000 cm/day for Si from its solution in Au-Si alloy as proposed by Hein seem unreasonably high. Also, the values of 30 mm/day for CdIn_2Te_4 and YIG may appear to be high, but higher temperature gradient or other favorable conditions could have made higher growth rates possible.

The relative advantages of RF and electrical resistance heating may be compared from the following point of view. If the ratio of electrical conductivity of solvent is high compared to the material to be grown, then heat generation within the solution may be higher in RF heating than in resistance heating. Temperature control will certainly be more difficult; however, convection within the solution zone will be enhanced.

The growth of SiC from Cr, GaP, and Ga(As, P) from Ga solvent by means of RF heating has proved advantageous (9, 10, 14, 20). RF heating was also used for the growth of materials such as ZnO (23), titanates, and titanates-zirconates (25). Because of their reactivity with quartz or other container materials, sealed Pt crucibles that coupled directly (Fig. A-6) or by means of a Pt susceptor ring to RF current were used. Sealing of the Pt crucibles by welding was especially important in ZnO growth in order to prevent the evaporation of the PbF_2 solvent. In other cases, tubular peripherally grooved graphite susceptors have been used for the growth of SiC, GaP, and Ga(As, P) to increase axial temperature gradients.

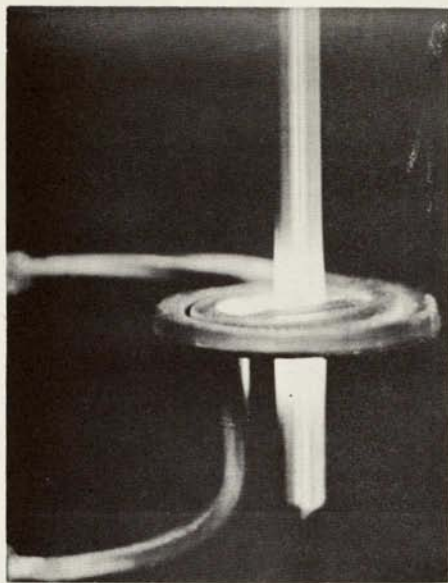


Fig. A-6. THM growth of ZnO from molten PbF_2 by RF coupling to sealed Pt crucible

Electrical resistance heating of the solution zone, with or without a fore- and after-heater, was used successfully for a great number of materials. Temperature control is more reliable. For a vertical furnace, the sealed crystal growth charge is best moved through its hot zone by means of a synchronous motor. The charge is thus simply lowered by means of a wire wound around the shaft of the motor. Figs. A-7 and A-8, respectively, show crystals of HgTe and CdCr_2Se_4 which have been grown in this way.

It should be noted that in the cases where the feed material is not in the form of a solid ingot, as growth proceeds the voids in the material gradually accumulate in the vicinity of the solvent zone region causing the elongation of the solution. This in turn results in a decrease of the cross section of the solution zone at its center region. This condition does not appear to have any detrimental effect on the crystal growth of materials in which one of the elemental components has a sufficiently high vapor pressure at the growth temperature. Under these conditions, the diffusion of the element into the solvent can occur via the vapor phase and across the void space next to the solution. In this way, the necessary concentration of solute in the solution is maintained during crystal growth. These conditions prevailed, specifically, in the crystal growth of HgTe and (Zn,Hg)Te when porous or powder feed material was used.

The same effect, namely, the narrowing of the solution zone, results in porous growth in the case of materials such as CdTe and CdCr_2Se_4 for which the vapor pressures of the elements are not sufficient for the evaporation and vapor phase diffusion from hot to cool parts of the solution zone to take place. Under these conditions, the restriction in the cross section of the solvent zone unavoidably reduces the amount of diffusing feed material through the solvent. Since, as a consequence, the effective growth rate decreases, crystal growth may not proceed properly. Porous ingots may be obtained or growth may cease completely.

Because of the importance of single crystal films in device application, an attempt has been made to grow thin films of BaTiO_3 by means of a two-dimensional version of THM (30). The experiment was unsuccessful with respect to its original objective; the results, however, showed clearly that this particular approach was sound in principle. The method will therefore be described briefly.

First, a thin film of 50 to 125μ thickness of CP BaTiO_3 powder was deposited on a clean 0.075 by 2.5 by 2.5 cm Pt sheet and sintered at 1300°C (see Fig. A-9).

An infrared (focusing) line heater was then used to move a strip of $\text{BaO:2B}_2\text{O}_3$ flux solvent from one end of the Pt substrate sheet across the film at a rate of 8.4 cm/day. Some of the experiments proved successful in that crystal films were produced that were single crystals in toto or in part. The composition and structure of the resulting single crystal material had not as yet been identified clearly.

SUMMARY

Crystal growth by the travelling heater method (THM) has certain advantages over melt or vapor growth for solid solutions, peritectic compounds, or incongruently evaporating materials. This method is similar to zone melting, except that a solvent zone instead of a molten zone is moved through the solid feed material.

The resulting growth and maximum travel rate of the solution zone heater are limited by the rate of transport of the most slowly diffusing molecular species across the solution zone. In this type of growth, constitutional supercooling is avoided by heating the center of the solution zone beyond a critical peak temperature.

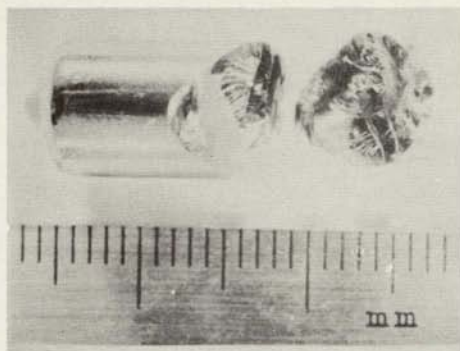


Fig. A-7. Single crystal of HgTe grown from solution in Te (crystal is cleaved)

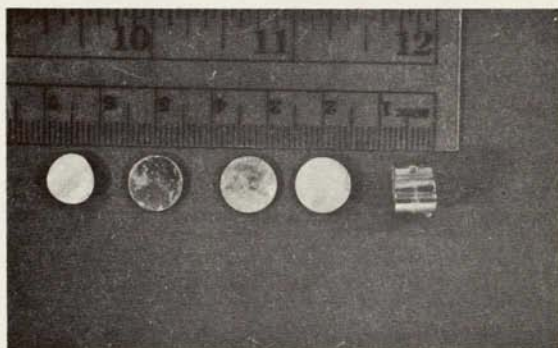


Fig. A-8. Crystal of CdCr_2Se_4 grown from CdCl_2 solution without seeding (crystal contains five to six grains)

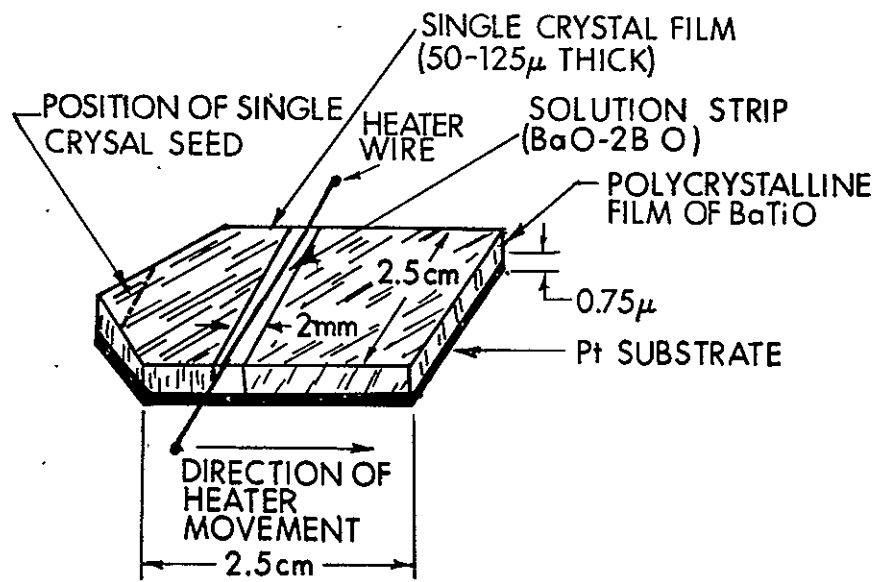


Fig. A-9. Schematic of experimental arrangement for thin film growth by variant of THM

In the growth of crystals of solid solutions, a stable convex or concave growth front profile could occur, even with a flat isotherm.

To date, a variety of materials of different properties and electronic applications have been grown by THM including Ga(As,P), (Hg,Zn)Te, ZnO, (Pb,Sr)TiO₃, CdCr₂O₄, and others. Most materials grown by this technique used a feed made from the prefabricated compounds, but often crystals can also be obtained by THM by direct synthesis and growth from a stoichiometric feed mixture of elemental or chemical constituents.

Single crystal thin films have also been prepared by a modified technique using a traveling radiation heater.

ACKNOWLEDGMENT

This program was funded under Contract NAS 12-2044 of the Electronics Research Center, National Aeronautics and Space Administration, Cambridge, Massachusetts, with Dr. J. D. Childress, CTM, as the Technical Monitor. Work also included in this outline was supported in part under Contracts DAAK 02-69-C-0071, Night Vision Laboratory, U. S. Army Electronic Command, Fort Belvoir, Virginia, and NOO 140-67-C-0386, U. S. Navy Underwater Sound Laboratory, Fort Trumbull, Connecticut, or as reported in the references.

LITERATURE CITED

1. Mlavsky, A. I., and Weinstein, Martin, J. Appl. Phys., 34, 2885 (1963).
2. Griffiths, L. B., and Mlavsky, A. I., J. Electrochem. Soc., 111, 305 (1964).
3. Wolff, G. A., and Mlavsky, A. I., Proc. Intern. Conf. on Adsorption and Crystal Growth, Nancy, France, No. 152, 339, 711 (1965).
4. Nuese, C. J., Tietjen, J. J., Gannon, J. J., and Gossenberger, H. F., TMS-AIME, 242, 400 (1968).
5. Gilman, J. J., "The Art and Science of Growing Crystals," John Wiley and Sons, Inc., New York (1963).
6. Nelson, H., RCA Review, 24, 683 (1963).
7. Dennis, J., and Henisch, H. K., J. Electrochem. Soc., 114, 263 (1967).
8. Wolff, G. A., Hebert, R. A., and Broder, J. D., Proc. Intern. Colloquium on Semiconductors and Phosphors, Garmisch, 1956; Interscience, N. Y., 547, (1958).
9. Wolff, G. A., LaBelle, Jr., H. E., and Das, B. N., TMS-AIME, 242, 436 (1968).
10. Wolff, G. A., Das, B. N., Lamport, C. B., Mlavsky, A. I., and Trickett, E. A., Mat. Res. Bull., 4, S67 (1969).
11. Weinstein, Martin, LaBelle, Jr., H. E., Mlavsky, A. I., J. Appl. Phys., 37, 2913 (1966).
12. Wolff, G. A., and Das, B. N., J. Electrochem. Soc., 113, 299 (1966).
13. Mason, D. R., and Cook, J. S., J. Appl. Phys., 32, 475 (1961).
14. Broder, J. D., and Wolff, G. A., J. Electrochem. Soc., 110, 1150 (1963).
15. Panish, M. B., and Sumski, S., J. Phys. Chem. Solids, 30, 129 (1969).
16. Hein, C. C., U. S. Patent 2,747,196 to Westinghouse Electric Corp. (May 29, 1956).

17. Goodman, C. H. L. , Research, 7, 168 (1954).
18. Abernethy, L. L. , Ramsey, T. H. , and Ross, J. W. , J. Appl. Phys. , 32, 376S (1961).
19. Pfann, W. G. , "Zone Melting, " John Wiley and Sons, Inc. , New York (1966).
20. Plaskett, T. S. , Blum, S. E. , and Foster, L. M. , J. Electrochem. Soc. , 114, 1304 (1967).
21. Hemmat, N. , Lamport, C. B. , Menna, A. A. , and Wolff, G. A. , Proc. ACCG Conf. on Crystal Growth, p. 79 (1969).
22. Bell, R. C. , Hemmat, N. , and Wald, F. , phys. stat. sol. (a), 1, 375 (1970).
23. Wolff, G. A. , and LaBelle, Jr. , H. E. , J. Am. Ceram. Soc. , 48, 441 (1965).
24. Perner, B. , J. Crystal Growth, 6, 86 (1969).
25. DiBenedetto, B. , and Cronan, C. J. , J. Am. Ceram. Soc. , 51, 364 (1968).
26. Tiller, W. A. , Jackson, K. A. , Rutter, J. W. , and Chalmers, B. , Acta Met. , I, 428 (1953).
27. Weinstein, Martin, and Mlavsky, A. I. , J. Appl. Phys. , 35, 1892 (1964).
28. Dismukes, J. P. , and Ekstrom, L. , TMS-AIME, 233, 672 (1965).
29. Yim, W. M. , and Dismukes, J. P. , J. Phys. Chem. Solids, 28, S187 (1967).
30. DiBenedetto, B. , and Wolff, G. A. , Appendix 6, Technical Report ECOM-00413-F, U. S. Army Electronics Command, Fort Monmouth, N. J. , December 1968.

Appendix B

ON SOLUTION AND TRAVELLING SOLVENT ZONE GROWTH OF
SEMICONDUCTING COMPOUNDS AND SOLID SOLUTIONS

N. H. Hemmat, C. B. Lamport, A. A. Menna, and G. A. Wolff

Abstract of Paper Presented at ACCG Conference on Crystal Growth,
August 11 to 13, 1969,

National Bureau of Standards, Gaithersburg, Maryland.
Published in Proc. ACCG Conference on Crystal Growth, Gaithersburg, Maryland,
August 1969, p. 79.

Work included in this outline was also supported in
part under Contracts DAAKO2-69-C-0071, Night
Vision Laboratory, U. S. Army Electronics
Command, Fort Belvoir, Virginia, and
N00-140-67-C-0338, U. S. Navy Underwater Sound
Laboratory, Fort Trumbull, Connecticut.

In the growth of solid solutions involving limited (dopant) or massive substitution, concentration gradients within the crystals produced cannot easily be avoided. In this case the passage of a solvent zone can be successfully applied. This technique (THM) is similar to floating zone growth except that the molten zone is replaced by a solution zone. The growth rate (also the critical maximum travel rate of the solution zone heater) producing uniform composition is generally governed by the limiting diffusion rate of the most slowly diffusing molecular species across the solution zone. It is important to heat the center of the solution zone above a critical temperature with respect to both solution-crystal interfaces (i. e., solution-feed material and solution-seed crystal interfaces) in order to avoid constitutional supercooling.

In the growth of cylindrical crystals of solid solutions, growth (and solution) front perturbations may be sustained, thus promoting a stable steady-state and axially symmetrical growth front geometry. This may be true even for flat isotherms. The combined effect of solidus-liquidus separation and differences in molecular diffusion rates are made responsible for this behavior.

THM growth of Ga(As, P), (Ga, Al)As, (Ga, In)P is described and compared with the growth of their solid solution end members, and of CdCr₂Se₄.

Appendix C
ANALYSIS OF CRYSTAL ORIENTATION

G. A. Wolff

One is often faced with the task of evaluating the results of early polycrystalline growth runs for the purpose of promoting single crystal growth. This is mostly done to elucidate the preferred direction of crystal growth, the cause of twinning, and interface stability. Such information is useful to improve conditions for single crystal growth.

Often, only two crystal grains have grown across the rod, but a large number of slices, including slices that are cut normal to the growth direction or parallel to it, must be checked for the orientation of their crystal grains. The Laue X-ray analysis is an accepted method for this task. It must be said, however, that the Laue method is excellent but time consuming and laborious when a large number of crystals have to be tested.

It is suggested that etching methods and/or the tracing of twin boundaries may be utilized to advantage. In sphalerite structure materials such as GaP, InP, or their solid solutions [and also in most other face-centered cubic materials such as materials of Al(Al), Al₄(Si), Cl(Mg₂Sn), H₁₁(CdCr₂Se₄) and other structures], all first-order twin boundaries are parallel to $\pm\{111\}$ planes. If several parallel traces of $\pm\{111\}$ are recognizable on a particular slice or surface of a cut, one can be certain that this trace on the viewed plane corresponds to a $\pm\{111\}$ twin trace. For its direction, the equation $u + v + w = 0$ (\vec{u} , \vec{v} , \vec{w} corresponding to orthogonal lattice vectors) is true. If a second twin trace can be observed adjacent to the same grain, its orientation is determined in principle. There are no twins of higher order than four. Consequently, there is only a limited number (less than seven) of flat twin interface boundaries or their straight line surface traces. Usually, only twin boundaries tend to exist as such extended straight lines. The greater the number of twin traces observed (and their respective angles known), the easier will be the analysis of the orientation of the various grains.

The use of preferential etching or mechanical abrading further facilitates this task by exposure of the twin plane intercepts with the surface of the crystal. This information can thus be obtained easily. A more general description of this theory follows.

A given crystal surface of orientation (hkl) may be intersected by a set of four $\{\bar{1}\bar{1}\bar{1}\}$ planes: $(\bar{1}\bar{1}\bar{1})$, $(1\bar{1}\bar{1})$, $(\bar{1}1\bar{1})$, and $(\bar{1}\bar{1}1)$. These planes may be either twin planes [in which case many parallel traces may intersect the (hkl) surface] or they could be stable planes of etch pits intersecting with the (hkl) crystal slice surface.

Since the interfacial angle and the relative symmetry between any two planes of the set of four tetrahedral $\{\bar{1}\bar{1}\bar{1}\}$ planes [$(\bar{1}\bar{1}\bar{1})$, $(1\bar{1}\bar{1})$, $(\bar{1}1\bar{1})$, and $(\bar{1}\bar{1}1)$] are identical, Eq. (C-1) may be

derived for all possible interfacial angles between two such $\{\bar{1}11\}$ planes on the one hand, and with a given (hkl) plane on the other. Here, (hkl) may represent a crystal plane which could be parallel to the surface of a crystal slice or normal to the growth direction.

If the reference plane $(hkl)_o$ of a cubic crystal is intersected by the planes $(hkl)_1$, $(hkl)_2$ --- $(hkl)_i$ --- $(hkl)_j$, then the cosine of the angle between the vector \vec{r}_{oi} [in other words, the vector representing the line of intersection with $(hkl)_i$]

$$\vec{r}_{oi} = \begin{vmatrix} h_o & k_o & \ell_o \\ h_i & k_i & \ell_i \end{vmatrix} = \left(\begin{vmatrix} k_o & \ell_o \\ k_i & \ell_i \end{vmatrix}, \begin{vmatrix} \ell_o & h_o \\ \ell_i & h_i \end{vmatrix}, \begin{vmatrix} h_o & k_o \\ h_i & k_i \end{vmatrix} \right) = (\vec{u}_{oi}, \vec{v}_{oi}, \vec{w}_{oi}) \quad (C-1)$$

and $\vec{r}_{oj} = (\vec{u}_{oj}, \vec{v}_{oj}, \vec{w}_{oj})$, [that is, the vector representing the line of intersection $(hkl)_j$] is given by

$$\cos(\vec{r}_{oi}, \vec{r}_{oj}) = \cos \left(\begin{vmatrix} h_o & k_o & \ell_o \\ h_i & k_i & \ell_i \end{vmatrix}, \begin{vmatrix} h_o & k_o & \ell_o \\ h_j & k_j & \ell_j \end{vmatrix} \right) \quad (C-2a)$$

$$= \frac{\begin{vmatrix} h_o & k_o & \ell_o \\ h_i & k_i & \ell_i \end{vmatrix} \cdot \begin{vmatrix} h_o & k_o & \ell_o \\ h_j & k_j & \ell_j \end{vmatrix}}{\left(\begin{vmatrix} h_o & k_o & \ell_o \\ h_i & k_i & \ell_i \end{vmatrix}^2 \cdot \begin{vmatrix} h_o & k_o & \ell_o \\ h_j & k_j & \ell_j \end{vmatrix}^2 \right)^{1/2}}$$

$$= \frac{A_{oo}A_{ij} - A_{oi}A_{oj}}{\left[(A_{oo}A_{ii} - A_{oi}^2)(A_{oo}A_{jj} - A_{oj}^2) \right]^{1/2}} \quad (C-2b)$$

$$= \frac{\cos[(hkl)_i, (hkl)_j] - \{\cos[(hkl)_o, (hkl)_i]\} \cdot \{\cos[(hkl)_o, (hkl)_j]\}}{\{\sin[(hkl)_o, (hkl)_i]\} \cdot \{\sin[(hkl)_o, (hkl)_j]\}} \quad (C-2c)$$

The expressions A_{oo} , A_{oi} , and A_{ij} denote $(h_o^2 + k_o^2 + \ell_o^2)$, $(h_o h_i + k_o k_i + \ell_o \ell_i)$, and $(h_i h_j + k_i k_j + \ell_i \ell_j)$, respectively. The remaining values A_{ii} , A_{jj} , and A_{oj} are defined correspondingly.

Setting $(hkl)_1 \equiv (1\bar{1}1)$ and $(hkl)_j \equiv (11\bar{1})$, and deleting the suffix in $(hkl)_o \equiv (hkl)$, Eq. (C-2) simplifies to

$$\cos(\vec{r}_{oi}, \vec{r}_{oj}) = - \left\{ \left(1 + \frac{k^2 + \ell^2}{h^2 + k\ell} \right)^2 - h^2 \left(\frac{k - \ell}{h^2 + k\ell} \right)^2 \right\}^{-1/2} \quad (C-3)$$

Thus, the angle, α , between both intersections for major reference planes (hkl) is

(hkl)	$(100), (0\bar{1}1)$	$(101), (110), (\bar{1}01), (\bar{1}10)$	(111)	(011)	$(001), (010)$
α	$0^\circ (180^\circ)$	$54^\circ 44' (135^\circ 16')$	$60^\circ 120^\circ$	$70^\circ 32' (109^\circ 28')$	90°

Where the determination of two such angles can be made, one is then able to determine in turn the general orientation of a crystal grain exposed on the wafer surface. In Si, Ge, and III-V compounds, the various crystals have twin neighbors with their common {111} twin composition plane visibly intersecting the surface. If the surface plane $(hkl)_I$ and the orientation of one of the twins (i. e. , twin no. I) have been determined, and if from experimental inspection their composition and twin plane is obviously $(11\bar{1})$, the surface plane $(hkl)_{II}$ of the other twin (i. e. , twin no. II) is then given by

$$\begin{bmatrix} h \\ k \\ l \end{bmatrix}_{II} = \frac{1}{3} \begin{bmatrix} \bar{1} & 2 & \bar{2} \\ 2 & \bar{1} & \bar{2} \\ \bar{2} & \bar{2} & \bar{1} \end{bmatrix} \cdot \begin{bmatrix} h \\ k \\ l \end{bmatrix}_I \quad (C-4)$$

This procedure can be extended in a corresponding manner to all crystals within a crystal slice if sufficient twinning occurs (as is mostly true in III-V compounds).

Appendix D
ELECTRICAL CONTACTING

S. C. Foote

In general, the conventional preparation of ohmic contacts to a III-V compound electro-luminescent diode (e. g. , sputtering or evaporation of a metallic film) is difficult for the following reasons.

1. The height of the metal-semiconductor potential barrier cannot be varied significantly by the choice of the metal, since the barrier height is primarily dependent on surface states of the semiconductor. ⁽¹⁾
2. The differing chemical and physical characteristics of A {111} and B { $\bar{1}\bar{1}\bar{1}$ } faces, among other orientations of the crystals, make contacting on one face of the diode an entirely different problem from contacting on the opposite face.
3. The temperature of operation of the diode limits the choice of the contacting material. This eliminates those materials that (1) melt at low temperatures or form a low melting point eutectic with the semiconductor, (2) have high diffusion rates into the semiconductor at or below the operating temperature, or (3) have coefficients of thermal expansion very much greater or less than that of the semiconductor material in question.
4. The alloying procedure necessary for contact adhesion in some processes induces dislocations in the interfacial region which can migrate into the semiconductor and thus degrade device performance.

Current contacting procedures fail to solve all of these problems. Therefore, in considering making contacts to $\text{Ga}_x\text{In}_{1-x}\text{P}$ electroluminescent diodes, we have arrived at a novel approach which promises to eliminate the problems outlined above.

The validity of the proposed contacting approach rests on the following facts.

1. The lattice parameters of $\text{Ga}_x\text{In}_{1-x}\text{P}$ solid solutions over a broad range of compositions ($0.506 \leq x \leq 1.00$) can be matched by suitable Si-Ge solid solutions (see Fig. D-1). Therefore, an excellent epitaxial fit should exist between a certain $\text{Ga}_x\text{In}_{1-x}\text{P}$ single crystal and an $\text{Si}_y\text{Ge}_{1-y}$ layer of appropriate composition, where

$$y = 1.837x - 0.9288 \quad \text{(D-1)}$$

2. Metal-germanium and metal-silicon compounds (germanides and silicides, respectively) possess both a high thermal and electrical conductivity³⁻⁵ as well as high melting points,⁽⁸⁾ and low reactivities.

*p 50 missing
in original*

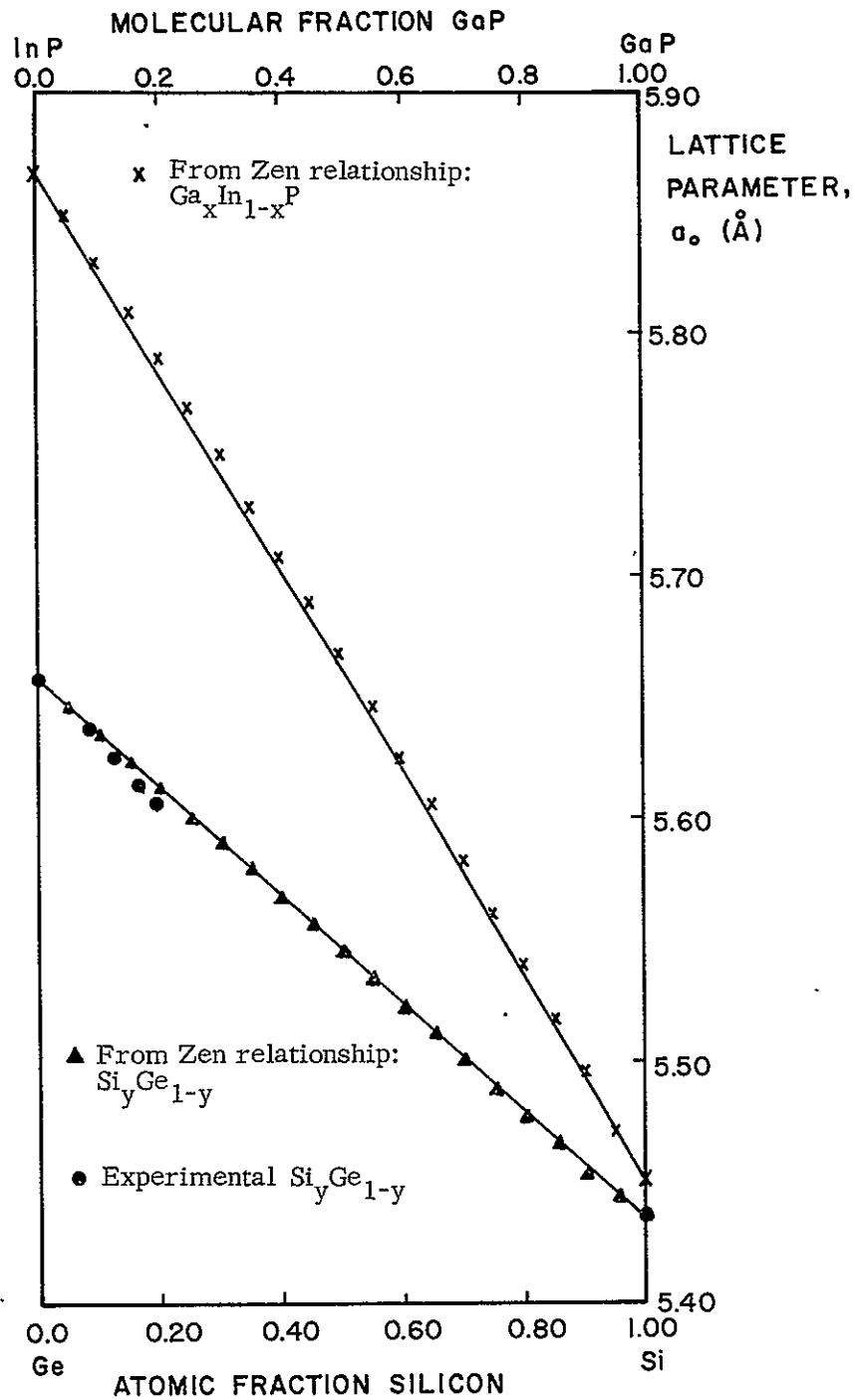


Fig. D-1. Lattice parameter variation with composition for $Ga_x In_{1-x} P$ and $Si_y Ge_{1-y}$

The contacting method envisioned consists first of the epitaxial deposition of $\text{Si}_y\text{Ge}_{1-y}$ on $\text{Ga}_x\text{In}_{1-x}\text{P}$. This will be done from a solution of Ge and Si in bismuth. Bismuth impurities will make the resultant $\text{Si}_y\text{Ge}_{1-y}$ layer highly n-type. At the operating temperature of the diode, the layer should be completely degenerate. Over this epitaxial layer a metal such as Pd or Pt will be deposited by evaporation or sputtering. A solid state reaction between the Si-Ge and the metal will be enhanced by heat treatment at a temperature low enough to avoid melting in the contact area. It is believed that diffusion penetration of the $\text{Si}_y\text{Ge}_{1-y}$ and metal in the solid state will lead to a much more uniform contact structure than that which might be achieved by liquid regrowth methods.

The resultant contact would essentially be a graded structure which consists of a degenerate n-doped or temperature degenerate $\text{Si}_y\text{Ge}_{1-y}$ layer directly on $\text{Ga}_x\text{In}_{1-x}\text{P}$, and a second layer of germanides and silicides of the deposited metal. Topping the contact will be a layer of the deposited metal, suitable for soldering to a lead (Fig. D-2). It is hypothesized that the basic contacting problems mentioned above would be solved for the following reasons.

1. The presence of surface states at the $\text{Ga}_x\text{In}_{1-x}\text{P}$ surface due to the termination of the bulk lattice should be eliminated. The $\text{Si}_y\text{Ge}_{1-y}$ solid solutions and the metallic germanides and silicides are all good conductors. Hence, the contact structure as a whole should have a low resistance and be nonrectifying.
2. The epitaxial deposition of the Si-Ge solid solution will eliminate the distinction between A {111} and B { $\bar{1}\bar{1}\bar{1}$ } faces of the semiconductor in electrical contacting.
3. The components of the contact and the resulting compounds have high melting points.
4. The precise matching of lattice parameters at the $(\text{Si}_y\text{Ge}_{1-y})$ ($\text{Ga}_x\text{In}_{1-x}\text{P}$) interface and the strain-free contact structure will eliminate dislocations at the interface or within the contact.

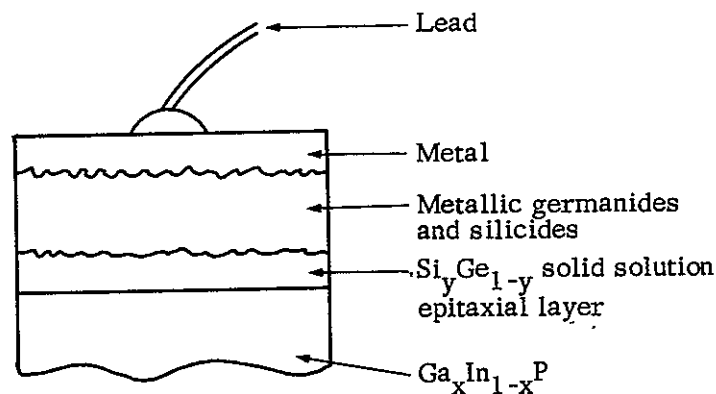


Fig. D-2. Proposed contact structure

LITERATURE CITED

1. Mead, C. A. : Ohmic Contacts to Semiconductors. *Solid-State Electronics*, 9, 1966, p. 1023.
2. Zen, E-an: Validity of Vegard's Law. *Amer. Mineralogist*, 41, 1956, p. 523.
3. Anderson, R. L. : Germanium-Gallium Arsenide Heterojunctions. *IBM Journ. Rev. Dev.*, 4, 1960, p. 283.
4. Nicoll, F. H. , The Use of Close-Spacing in Chemical-Transport Systems for Growing Epitaxial Layers of Semiconductors. *J. Electrochem. Soc.*, 110, 1963, p. 1165.
5. Fang, F. F. , and Howard, W. E. : Effect of Crystal Orientation on Ge-GaAs Heterojunctions. *J. Appl. Phys.*, 35, 1964, p. 612.
6. Samsonov, G. V. : High Temperature Materials, #2 Properties Index. Plenum Press N. Y. , 1964.
7. Hansen, M. : Constitution of Binary Alloys. McGraw-Hill Book Co. , N. Y. , 1958.
8. Hession, F. X. , Goss, A. J. , and Trumbore, F. A. : Ge-Si Phase Diagram. *J. Phys. Chem.*, 59, 1955, p. 1118.